RNA-Seq data analysis of a rodent model of adolescent binge drinking reveals pathways and candidate genes involved in neuronal remodeling and neuroimmune activation

Alejandro Q. Nato, Jr.[1,†], Hafiz Ata Ul Mustafa[1*], Riya K. Patel[1*], Hannah G. Sexton[1,2], Scott D. Moore[3,4], James Denvir[1], Donald A. Primerano[1], and Mary-Louise Risher[1,2,3,†]

[1]Department of Biomedical Sciences, Joan C. Edwards School of Medicine, Marshall University, Huntington, WV, USA

[2]Hershel 'Woody' Williams Veteran Affairs Medical Center, Huntington WV, USA

[3]Department of Psychiatry and Behavioral Sciences, Duke University Medical Center, Durham, NC, USA

[4]Durham Veteran Affairs Medical Center, Durham, NC, USA

*equal contribution

[†]**Addresses for correspondence:**

Alejandro Q. Nato, Jr., 1700 Third Ave (BBSC 336M), Huntington, WV 25755

Tel: 304 6963562 Fax: 304 6967207 Email: nato@marshall.edu

Mary-Louise Risher, 1700 Third Ave (BBSC 336L), Huntington, WV 25755

Tel: 304 6963894 Fax: 304 6967207 Email: risherm@marshall.edu

Running titles: Identification of candidate genes for alcohol use disorder using RNA-seq data; Pathway functional and network enrichment analyses of RNA-Seq data in alcohol use disorder

Keywords: bioinformatics, complex traits, computational tools, identification of disease genes, RNA-seq, remodeling, neuroimmune activation, neuroinflammation, addition, receptor function, K^+ channels

Email addresses of authors:

Alejandro Q. Nato, Jr.: nato@marshall.edu

Hafiz Ata Ul Mustafa: ataulmustafa@marshall.edu

Riya K. Patel: patel238@marshall.edu

Hannah G. Sexton: sextonh@marshall.edu

Scott D. Moore: sdmoore@duke.edu

James Denvir: denvir@marshall.edu

Donald A. Primerano: primeran@marshall.edu

Mary-Louise Risher: risherm@marshall.edu

ABSTRACT

Introduction: Alcohol use disorder (AUD) is a complex, chronic psychiatric disease. AUD manifests as having uncontrollable drinking patterns with detrimental effects. Excessive alcohol intake in the form of binge drinking, which is common among adolescents and young adults, is associated with increased risk of developing AUD. Here, we analyze RNA-seq data from hippocampi of Sprague Dawley rats to investigate temporal changes in gene expression. We used a rodent model of binge drinking, i.e., adolescent intermittent ethanol (AIE), to identify candidate genes that may play a role in the chronic changes in brain function and contribute to the development of AUD.

Methods: At postnatal day (PND) 30 (adolescence), rats received chronic intermittent ethanol (5g/kg intragastrically (i.g.) 10 times across 16 days). We extracted total RNA from rat hippocampal tissue that was collected at three time points. RNA was sequenced on an Illumina HiSeq 2000 platform. We processed RNA-seq data (TrimGalore), compiled gene counts (HTSeq), and performed differential expression analysis (DESeq2). The full rank list of genes and the differentially expressed genes (DEGs) with nominal $p<0.05$ were used as inputs for pathway-based enrichment analyses GSEA and Cytoscape, respectively, at 3 timepoints in the presence or absence of ethanol (i.e., 3 comparisons). For each of these comparisons, GSEA was used to identify genes involved in enriched Gene Ontology (GO) terms while Cytoscape and its apps were used to identify networks of genes and, subsequently, subnetworks (i.e., clusters) of genes enriched by higher interaction. From clusters containing 15 or more nodes, we prioritized genes related with particular functions, cell types, or diseases, which were present in GO

Processes, Kyoto Encyclopedia of Genes and Genomes (KEGG) Pathways, or Reactome Pathways.

Results: Based on GSEA, the most impacted differential gene expression occurs within the potassium channels and receptor function but is heavily dependent on the time point at which the analysis occurs. Across both GSEA and Cytoscape pathway analyses, the most striking changes occur in genes that regulate neuroinflammatory processes and neuronal/synaptic remodeling and coincide with the enrichment of pathways involved in addiction processes.

Conclusion: Identification of genes dysregulated by AIE may be useful in determining the underlying mechanism for acute and chronic effects of AIE exposure that contribute to neuronal remodeling and increased risk of developing AUD.

INTRODUCTION

Alcohol misuse is a major and critical public health issue with high economic impact. It costs the United States ~$249 billion annually (Sacks et al., 2015) in terms of loss of workplace productivity, hospitalizations for acute and chronic alcohol-related injury and disease, and costs relating to the criminal justice system. Approximately 3 million people worldwide (2016 data) and about 88,000 people in the USA (2011-2015 data) die annually from harmful use of alcohol, which represent 5.3% and 28.1% of all deaths, respectively. Alcohol is thus one of the major leading preventable causes of death (third in the USA), with 13.5% of all global deaths between the ages 20-39 attributable to alcohol use (Centers for Disease Control and Prevention, 2019; World Health Organization, 2018). Alcohol consumption typically begins in adolescence with 90% of alcohol being consumed in a binge drinking manner (NIAAA, 2020; U.S. DOJ, 2005). High prevalence of binge drinking coincides with late stage brain maturation and a period in which select brain regions are highly vulnerable to the cytotoxic effects of ethanol and other drugs of abuse (Harper & Matsumoto, 2005). Growing evidence from epidemiological studies reveals that early onset (13-18 years of age) binge drinking is associated with increased likelihood of developing an alcohol use disorder (AUD) (Chin et al., 2010; DeWit et al., 2000; Grant & Dawson, 1997; Hanson et al., 2011) and the emergence of cognitive deficits in verbal and non-verbal skills, attention, visuospatial function, and learning (Chin et al., 2010; Hanson et al., 2011; Tapert et al., 2002; Tapert & Brown, 1999). AUDs are globally ranked as one of the most frequent mental disabilities and are related to several other physical and nervous system disorders (Hasin et al., 2007; Rehm, 2011; Rehm et al., 2015). AUD may result in mental health problems and economic problems for individuals and could have harmful impacts on their families, relatives, colleagues and the society in terms of violence, vehicle accidents, and

criminal offenses (Rehm et al., 2009). Over the last decade, concerted efforts have been made to understand the direct contributions of adolescent onset binge drinking to long-lasting changes in neuronal structure, function and subsequent cognitive changes that may be associated with the emergence of AUD.

Parallels between human findings and rat models of binge drinking, which are consistent across laboratories, are emerging (Crews et al., 2019; Spear, 2016; Spear & Swartzwelder, 2014b). Adolescent intermittent ethanol exposure (AIE) is a major predictor for AUD development that substantially affects neuronal function by causing aberrant hippocampal structure and function (Kim et al., 2019; Risher et al., 2013; Risher et al., 2015b). These changes correlate with select hippocampal-dependent deficits in learning processes that persist into adulthood (Acheson et al., 2013; Coleman et al., 2014; Risher et al., 2013; Vetreno & Crews, 2015). These behavioral deficits coincide with enduring enhancement of long-term potentiation (LTP) and the persistence of neuronal hyperexcitability (Fujii et al., 2008; Risher et al., 2015a; Sabeti & Gruol, 2008; Swartzwelder et al., 2016), which are indicative of neuronal remodeling. However, underlying mechanisms that drive the changes at the synaptic and circuit level remain somewhat elusive. Here, we analyze rat hippocampal gene expression profiles to understand the temporal changes that occur in response to repeated adolescent ethanol exposure with the goal of elucidating changes in gene regulation that contribute to synaptic and neuronal remodeling and the development of AUD.

MATERIALS AND METHODS (Read all)

Adolescent Intermittent Alcohol Exposure

We used Sprague Dawley rats (Rattus norvegicus) SPF grade, which were obtained from Hilltop Lab Animals (PA, USA). At postnatal day (PND) 30 (adolescence), 18 rats received chronic intermittent ethanol (5g/kg intragastrically (i.g.)) or water (H_2O) 10 times across 16 days (Risher et al., 2015b). Rats were anesthetized using isoflurane and then euthanized by decapitation. The brains were removed and the hippocampus was rapidly dissected and frozen. Hippocampal tissue was collected from 6 rats each at three time points: 1) 24 hours after 4th dose (PND35), 2) 24 hours after last dose (PND46), and 3) 26 days after last dose (PND70; adult). These timepoints correlate with adolescence (PND35 and PND46) and young adulthood (PND70) in humans (Sengupta, 2013).

RNA Extraction and Sequencing

We extracted total RNA from rat hippocampal tissue using RNeasy mini kit (Qiagen, Germantown, MD) following the manufacturer's instructions. RNA sample quantity and quality were determined using a NanoDrop 2000 (Thermo Fisher Scientific, Waltham, MA). We used the Roche Kapa mRNA Hyper prep kit (Indianapolis, IN) to prepare libraries following the manufacturer's instructions. Purified libraries were quantified using Qubit 2.0 Fluorometer (Life Technologies, Carlsbad, CA) and Agilent 2000 Bioanalyzer (Agilent Technologies, Santa Clara, CA). Clusters were generated by cBot with the purified library and sequenced on an Illumina HiSeq 2000 platform (Illumina, Inc., San Diego, CA). All sequencing was performed at the Sequencing and Genomic Technologies Service Center, Duke University, Durham, NC.

Differential Expression Analysis

We processed RNA-seq data using TrimGalore toolkit (Krueger, 2020), a Perl wrapper that employs Cutadapt (Martin, 2011) and FASTQC (Andrews, 2010) to reliably trim low quality bases and Illumina sequencing adapters from the FASTQ files. Reads that were at least 20 nucleotides in length were aligned and mapped to the Rnor 6.0v84 version of the rat genome and transcriptome (Kersey et al., 2012) using STAR (Dobin et al., 2013). Only reads that mapped to a single genomic location were included in subsequent analyses. Gene counts were compiled using HTSeq (Anders et al., 2015) and filtered to retain genes that had at least 10 reads in any given library. Normalization and differential expression analysis for comparisons at the three time points (PND35, PND46, and PND70) in the presence of EtOH vs. absence of EtOH, i.e., PND35 EtOH vs H_2O, PND46 EtOH vs H_2O, and PND70 EtOH vs H_2O, respectively, were performed using the DESeq2 Bioconductor package in R (Huber et al., 2015; Love et al., 2014; R Core Team, 2020). To control for multiple hypothesis testing, the false discovery rate (FDR) was calculated using the Benjamini-Hochbeerg method (Benjamini & Hochberg, 1995). Using all of the genes in each of conditions above (i.e., presence or absence of EtOH), genes were hierarchically clustered (unsupervised) by correlation distance with complete linkage. Heatmaps were generated using the differentially expressed genes (DEGs) with FDR$\leq$0.05.

Pathway-based Enrichment Analyses for Candidate Gene Identification

Gene Set Enrichment Analysis (GSEA)

GSEA (Mootha et al., 2003; Subramanian et al., 2005), which computationally assesses whether a defined set of genes statistically distinguishes the difference between two biological states, was performed to identify differentially regulated pathways and gene ontology (GO) terms by using

as input the full rank list of genes from the differential expression analysis as for each of the comparisons (PND35 EtOH vs H2O, PND46 EtOH vs H2O, and PND70 EtOH vs H2O). For this study, we focused on the part of GSEA that tested pre-defined gene sets from GO that grouped genes based on biological process and molecular functions.

Cytoscape pathway and functional enrichment analyses

To be a bit stringent yet permissive due to the small sample size, genes that reached nominal significance ($p<0.05$) through differential expression analysis at the three comparisons, were used as input for Cytoscape pathway analysis (v.3.7.2, Shannon et al. (2003)). To identify subnetworks (clusters) of genes that are functionally enriched by higher interaction (with minimum cluster size of 10 allowing up to 25 interactors), two Cytoscape apps (`clusterMaker` that implements the Markov CLustering Algorithm (MCL) and `StringApp`) were employed through automation using R (Doncheva et al., 2019; Morris et al., 2011; Otasek et al., 2019; R Core Team, 2020; Shannon et al., 2003). From these subnetworks, (1) we selected those that have at least 15 nodes, (2) subsequently filtered gene sets, which were functionally enriched in GO Processes, KEGG Pathways, or Reactome Pathways within Cytoscape (Ashburner et al., 2000; Jassal et al., 2020; Kanehisa, 2019; Kanehisa & Goto, 2000; Kanehisa et al., 2019; The Gene Ontology, 2019), and (3) further selected clusters that have genes involved in particular topics, i.e., functions, cell types, or diseases, which include: astrocytes, addiction, remodeling, immune response, synaptic/signaling, blood brain barrier, mitochondria, and aging. Genes that are present in at least three main topics (especially remodeling, immune response, and synaptic/signaling) were prioritized.

RESULTS

Differential Expression Analysis

Of the 15,772 genes analyzed, there were 12, 1, 1 differentially expressed genes (DEGs) with FDR≤0.05 (for heatmap generation) and 710, 1,076, and 239 DEGs with nominal $p<0.05$ (input for Cytoscape analysis) for PND35 EtOH vs H_2O, PND46 EtOH vs H_2O, PND70 EtOH vs H_2O, respectively (Supplementary File 1: S1_Differential_Expression.xlsx). Since 2 of the 3 comparisons (PND46 EtOH vs H_2O and PND70 EtOH vs H_2O) only had 1 DEG each using FDR≤0.05 threshold, only one heatmap was generated (Figure 1).

Pathway-based Enrichment Analyses for Candidate Gene Identification

GSEA

Here, we focused on the GSEA output involving enriched GO terms. After removal of duplicate entries, 15,678 of the 15,772 genes from differential expression analysis were used for GSEA. Of the gene sets retrieved from GO, 1,454 contained one or more of these 15,678 genes. Gene sets were initially filtered based on the number of members, i.e., gene set size (min=15, max=500), which resulted in selecting 935 gene sets (i.e., filtered out 519 gene sets). For each of the three comparisons, the top 15 upregulated and top 15 downregulated gene sets were assessed.

GSEA for PND35 EtOH vs H_2O (24 hours after the 4th dose): Earliest timepoint

For PND35 EtOH vs H_2O, 358 (38.2%) gene sets are upregulated, 7 (0.7%), 15 (1.6%), and 35 (3.7%) of which are significant at FDR<0.25, nominal $p<0.01$, and nominal $p<0.05$, respectively. On the other hand, 577 (61.7%) gene sets are negatively regulated, 25 (2.7%), 29 (3.1%), and 77

(8.2%) of which are significant at FDR<0.25, nominal p<0.01, and nominal p<0.05, respectively. Plots of top 20 enriched GO terms upregulated and negatively regulated are shown in Figures 2 and 3, respectively.

Enrichment in 4 of the top 15 upregulated gene sets involve mitochondrial ribosomal proteins ('mitochondrial ribosome', 'organellar ribosome', 'ribosomal unit', 'ribonucleoprotein complex'), while 2 of the top 15 show gene enrichment of endoplasmic reticulum components ('endoplasmic reticulum membrane' and 'endoplasmic reticulum part') and ion channel activity ('auxiliary transport protein activity' and 'channel regulator activity'). Within the 'auxiliary transport protein activity' and 'channel regulator activity' gene sets, multiple potassium (K^+) channel subunits, including the shaker subfamily were enriched (KCNAB2, KCNV1, KCNAB3, KCNS3, KCNAB1) (Supplementary Files 2 and 3: S2_PND35_GeneSet_1.txt and S3_PND35_GeneSet_2.txt, respectively). Other genes of interest include neuropeptide Y receptor 2 (NPY2R) and the FXR1 gene within the 'ribonucleoprotein complex' gene set.

When assessing negative regulation of genes at PND35, the most robust finding was that 5 of the top 15 gene sets downregulated were associated with the extracellular matrix ('extracellular matrix', 'extracellular matrix structural constituent', 'proteinaceous extracellular matrix', 'extracellular matrix part', 'collagen') and included the downregulation of laminins (LAMA1, LAMC1, LAMB1), collagens (COL4A4, COL9A2, COL18A1, COL13A1, COLQ, COL9A3, COL7A1, COL9A1, COL3A1, COL5A1, COL4A5), thombospondin (THBS4), tenascin XB (TNXB). On the other hand, 2 of the top 15 gene sets negatively regulated involved synaptic activity ('neurological system process' and 'system process') and were negatively regulated with regard to multiple K^+ channels (KCNMA1, KCNK5, KCNQ3, KCNK3, KCNQ4) (Supplementary Files 4 and 5: S4_PND35_GeneSet_3.txt and S5_PND35_GeneSet_4.txt,

respectively), glutamate receptors (GIRK2, GIRK1, GRM8), dopaminergic receptors (DRD1 and DRD 4), and the adenosine A2a receptor (ADORA2A). A number of genes were also negatively regulated within the 'transforming growth factor β receptor signaling pathway' and the 'transmembrane receptor protein serine threonine kinase signaling pathway' including 2 genes involved in transforming growth factor function (TGFBRAP1 and TGFBR3).

GSEA for PND46 EtOH vs H_2O (24 hours after the last dose)

For PND46 EtOH vs H_2O, 478 (51.1%) gene sets are upregulated, 73 (7.8%), 48 (5.1%), and 90 (9.6%) of which are significant at FDR<0.25, nominal p<0.01, and nominal p<0.05, respectively. On the other hand, 457 (48.9%) gene sets are negatively regulated, 146 (15.6%), 73 (7.8%), and 124 (13.3%) of which are significant at FDR<0.25, nominal p<0.01, and nominal p<0.05, respectively. Plots of top 20 enriched GO terms upregulated and negatively regulated are shown in Figures 4 and 5, respectively.

Enrichment in 13 of the top 15 gene sets upregulated involve genes important in receptor and ion channel activity. The top 2 gene sets were 'glutamate receptor activity' and 'glutamate signaling pathway'. The majority of enriched genes are designated as ionotrophic glutamate receptor subunits (GRIN2A, GRIN2B, GRIA2, GRIK3, GRIK2, GRIA1, and GRIK1), 3 of which are kainate receptors. However, some metabotrophic glutamate receptors were also enriched (GRM5, GRM3, and GRM7) along with gamma-aminobutyric acid (GABA) B receptor 1 (GABBR1). In the 'synaptic transmission' gene set the gene encoding for mGluR5 (GRM5) is enriched. This receptor is expressed on neurons and astrocytes in early development and is involved in regulation of glutamate availability (Isherwood et al., 2018). Six of the next 8 gene sets upregulated involved potassium ('potassium ion transport', 'voltage gated potassium

channel activity', 'potassium channel activity', and 'voltage gated potassium channel complex'), voltage gated channels (voltage gated channel activity' and 'voltage gated cation channel activity') and 'synaptic transmission'. In these gene sets, 26 genes involved in K^+ ion transport were enriched (not shown). KCNC4 was the most enriched and encodes for Kv3.4. This is a K^+ channel that is involved in cell death mechanisms. KCNJ10 is one particular gene that stands out that encodes the astrocyte K^+ channel Kir4.1 and is heavily involved in K^+ uptake in response to synaptic transmission. Dysregulation of Kir4.1 disrupts glutamate uptake by astrocytes (Kucheryavykh et al., 2007). KCNQ2 encodes for the protein Kv7.2. This is a slowly activating and deactivating potassium channel that plays a critical role in the regulation of neuronal excitability. The synaptic transmission gene sets ('voltage gated channel activity', 'voltage gated cation channel activity', 'transmission of nerve impulse', and 'monovalent inorganic cation transport') overlap extensively with the K^+ channel gene sets. However, they also reflect changes in a number of calcium channels (CACNB4, CACNB2, CACNA2D1, CACNB1, CACNA1H), chloride channels (CLCN3 and CLCN4), and sodium channels (SCN1B and SCN2B). CACNA2D1 gene enrichment is of particular interest since it is involved in astrocyte-induced synaptogenesis during development, throughout life, and is involved in aberrant synaptic/neuronal remodeling in response to injury. Moreover, previous work demonstrates the upregulation of the encoded protein α2δ-1 in response to AIE in CA1 hippocampus, albeit at a later time point (PND70) (Risher et al., 2015b; Swartzwelder et al., 2016). Homer homolog 1 (HOMER1), HOMER2, and neuroligin 1 (NLGN1) were also enriched at this time point. These genes are important for synaptogenesis, synaptic stabilization, astrocyte morphogenesis, and regulation of Ca^{2+} homeostasis at synaptic dendritic spines (Sala et al., 2005). 'Axonogenesis', 'neuron differentiation' and 'generation of neurons' show enrichment overlap in a number of

genes that are involved in synaptic and axonal remodeling (NLGN1, NTNG2, ROBO2, NRXN1, OPHN1). ROBO2 is involved in axon guidance, while Oligoprenin 1 drives RHOA activity and is involved in the growth and stabilization of dendritic spines. Netrin G2 is implicated in synaptic and circuit organization and once again is found to be more highly expressed in models of epilepsy (Pan et al., 2010). Thy1 is thought to play a role in cell-cell cell-ligand interactions during synaptogenesis (Liu et al., 1996). Other genes enriched in both the 'axonogenesis' and 'transmission of nerve impulse' are kallikrein 8 (KLK8), adhesion molecule with Ig-like domain 1 (AMIGO1), synaptotagmin I (SYT1), synapsin I and III (SYN1 and SYN3). Kallikrein 8 is intriguing because it is known to regulate long-term potentiation and therefore play a role in the regulation hippocampal-dependent memory processes.

In contrast, 8 of the top 15 gene sets negatively regulated include neuronal and synaptic remodeling-related terms ('proteinaceous extracellular matrix', 'extracellular matrix', 'extracellular matrix structural constituent', 'extracellular matrix part', 'extracellular region', 'collagen', 'extracellular region part', 'basement membrane'). They include genes associated with collagen (COL4A5, COL6A3, COL7A1, COL18A1, COL3A1, COL13A1, COL4A4, COLQ, COL9A2, COL5A3, COL9A1, COL5A1, COL4A3) and laminin (LAMA2, LAMAB2, LAMC1, LAMB1, LAMA4). Genes similarly regulated within 'carbohydrate binding', 'tissue development', 'pattern binding', and 'skeletal development' groups also made the top 15 gene set list and had significant gene overlap with regard to tissue remodeling. Other genes of interest that are negatively regulated in response to AIE are tenascin XB (TNXB) and periostin (POSTN), semaphorin 3A (SEMA3A), complement component 1q (C1Q), interleukin 1 beta (IL1B), lipopolysaccharide binding protein (LBP), chemokine (C-X-C motif) ligand 9 (CXCL9), interleukin 6 receptor (IL6R), tumor necrosis factor receptor 11β (TNFRSF11B), and kallikrein 6

(KLK6). Periostin is a neurite outgrowth-promoting factor (Matsunaga et al., 2015) that is upregulated in response to cerebral ischemia (Shimamura et al., 2012). Semaphorin 3A is involved in axon guidance. CXCL9 and IL6 can mediate activation of inflammatory pathways via the JAK/STAT3 pathway, driving astrocyte reactivity. Kallikrein 6 contributes to astrocyte reactivity (Scarisbrick et al., 2012), suggesting that negative regulation of these factors may be important for limiting cell damage induced by AIE-induced neuroinflammation. The 8th, 9th, and 15th on the gene set list of negatively regulated genes are 'ER-golgi intermediate compartment', 'cytokine binding', and 'I kappa kinase NF-κB cascade', respectively. The 'cytokine binding' gene set shows negative regulation of a number of interleukin receptors (ILR) and tumor necrosis factor receptors (TNFR) that are particularly important for neuroinflammatory processes, these include: IL12RB2, IL15R, IL9R, IL3RA, IL6R, IL10RB, IL2RG, IL13RA2, IL1R1, IL2RA, TNFRSF1B, TNFRSF1A, TNFRSF4, along with 3 genes for interferon gamma receptors (IFNGR2, IFNAR2, IFNAR1) (Supplementary File 6: S6_PND46_GeneSet_1.txt). The 'I kappa kinase NF-κB cascade' gene set shows some overlap with the 'cytokine binding' genes along with the addition of TRADD, TRAF2, CASP8, CARD10, TNFRSF1A, TNFRSF10B, TICAM2, CASP1, LITAF, that are all involved in the regulation of neuroinflammation and neuronal death cascades. Contrary to the negative regulation of neuroinflammation-related genes, RHOA is also negatively regulated within the 'I kappa kinase NF-κB cascade' group. Deletion of RHOA from microglia activates a pro-inflammatory cascade, disrupts neuronal function, and results in neurodegeneration (Socodato et al., 2020). However, its more well-known role is in dendritic remodeling (Fox et al., 2020).

GSEA for PND70 EtOH vs H_2O (26 days after the last dose)

For PND70 EtOH vs H_2O, 408 (43.6%) gene sets are upregulated, 16 (1.7%), 22 (2.4%), and 39 (4.2%) of which are significant at FDR<0.25, nominal p<0.01, and nominal p<0.05, respectively. On the other hand, 527 (56.4%) gene sets are negatively regulated, 3 (0.3%), 16 (1.7%), and 69 (7.4%) of which are significant at FDR<0.25, nominal p<0.01, and nominal p<0.05, respectively. Plots of top 20 enriched GO terms upregulated and negatively regulated are shown in Figures 6 and 7, respectively.

The negative regulation of tissue remodeling genes at PND46 (24 hour after the 10th dose) is almost completely reversed by PND70 (26th day washout). At PND70, 9 out of the top 15 gene sets upregulated are related to tissue remodeling ('contractile fiber part', 'extracellular matrix part', 'extracellular matrix structural constituent', 'collagen', 'proteinaceous extracellular matrix', 'extracellular matrix', integrin binding', 'tissue development', ''myofibril') and involve the collagens (COL4A5, COL16A1, COL18A1, COL13A1, COL6A3, COL5A3, COL3A1, COL5A1, COL4A3, COL5A2, COL7A1, COL4A2, COLQ, COL9A2, COL9A3, COL8A1), laminins (LAMC1, LAMB2, LAMA2, LAMA3), and tenascin XB (TNXB), thrombospondins (THBS4), ADAM metallopeptidase with thombospondin type motifs (ADAMTS 13, 23, 9), intercellular adhesion molecules (ICAM2), and Janus kinase 2 (JAK2). Also included in the top 15 genes sets enriched following washout involve 'exopeptidase activity', 'endonuclease activity', and 'transmembrane receptor protein tyrosine kinase activity'. Of particular interest is the enrichment of ephrin A4 (EFNA4), EPH receptor B2 (EPHB2), and neuropilin 1 (NRP1) within the 'transmembrane receptor protein tyrosine kinase activity' gene set. Neuropilin 1 is involved in cell migration. Ephrins are a group of receptor kinases that are anchored to the cell

membrane by glycosylphosphatidylinositol (GPI) or by a transmembrane domain. They are most commonly associated with synaptic development and synaptic remodeling.

Calcium/calmodulin-dependent protein kinase (CaM kinase) IIα (CAMK2A) was enriched in the 'regulation of transcription factor activity' and the 'regulation of DNA binding' gene sets. This gene is part of the serine/threonine protein kinases family and the Ca(2+)/calmodulin-dependent protein kinases subfamily. It is involved in the regulation of NMDAR-dependent potentiation of AMPAR, dendritic spine development, and mediates numerous downstream second messenger processes. The single immunoglobulin and toll-interleukin 1 receptor (TIR) domain (SIGIRR) was enriched within the 'regulation of transcription factor activity' and the 'regulation of DNA binding' gene sets. The Toll/IL-1 receptor (TIR) domain is involved in the regulation and activation of transcription factors that regulate proinflammatory cytokines (Narayanan & Park, 2015). Receptor (TNFRSF)-interacting serine-threonine kinase 1 (RIPK1), tumor necrosis factor superfamily, member 1A, 10, and 10B (TNFRSF1A, TNFRSF10 and TNFRSF10B), lipopolysaccharide-induced TNF factor (LITAF), caspase 8 (CASP8), Ras homolog gene family member A and C (RHOA and RHOC), and mindbomb homolog 2 (MIB2) were all enriched in the 'positive regulation of I kappa kinase NF-κB cascade' gene set and are all involved in neuroinflammation and/or cell death pathways.

On the other hand, 2 of the top 3 gene sets that are negatively regulated at PND70 are associated with neurotransmitter function ('neurotransmitter receptor activity' and 'neurotransmitter binding'). Most highly downregulated genes include a number of cholinergic (CHRNA7, CHRM3, CHRNA5, CHRNA4, CHRNE) and GABAergic receptors (GABRA3, GABRG2, GABRA4, GABRA2). Other receptor genes found to be significantly downregulated include CCKBR, BRS3, and DRD1. Moreover, 2 of the top 15 gene sets negatively regulated are

involved in potassium channel function ('voltage gated potassium channel activity' and 'voltage gated potassium channel complex') (Supplementary Files 7 and 8: S7_PND70_GeneSet_1.txt, and S8_PND70_GeneSet_2.txt, respectively). The potassium-related channels downregulated include: KCNH3, KCNJ5, KCNC4, KCNC1, KCNC1, KCNJ15, KCNJ4, KCNJ4, KCNA3, KCNA5, KCNH4, KCNA5, KCNMA1, and KCNB2. Voltage-gated potassium (Kv) channels represent the most complex class of voltage-gated ion channels from both functional and structural standpoints. Their diverse functions include regulating neurotransmitter release, heart rate, insulin secretion, neuronal excitability, epithelial electrolyte transport, smooth muscle contraction, and cell volume. They are present in both excitable and non-excitable cells. A number of channel protein genes within the delayed rectifier class that are known to mediate voltage-dependent potassium ion permeability of excitable membranes are negatively regulated and include: KCNC4 (Kv3.4), KCNA3 (Kv1.3), KCNA5 (Kv1.5), KCNA5 (Kv1.5), KCNB2 (Kv2.2) and KCNA3 (Kv1.3). KCNH3 (Kv12.2) is also downregulated. This is important because KCNH3 encodes for a protein that is involved in hippocampal excitability and epilepsy (Zhang et al., 2010). KCNJ5 (Kir3.4), KCNJ15 (Kir4.2) and KCNJ4 (Kir2.3) are inwardly rectifying potassium channels that are also important for neuronal signaling and membrane excitability. KCNC1 (Kv3.1) a gene that mediates the voltage-dependent potassium ion permeability of excitable membranes is also downregulated at this late timepoint. KCNMA1 (KCa1.1) encodes a BKCa channel that has a large conductance. It is a voltage and calcium-sensitive potassium channel which is fundamental for neuronal excitability. Loss of BKCa channel function results in neuronal hyperexcitability (N'Gouemo, 2014). Interestingly, it is also involved in the regulation of β1-integrin function and cell adhesion (Tanner et al., 2017).

Combined with the enrichment of many ECM genes provides additional evidence that AIE drives dysregulation of neuronal remodeling processes.

Furthermore, 18 out of 50 genes in the 'CAMP mediated signaling' gene set were negatively regulated whereas, 78 genes out of 240 were negatively regulated in the 'G protein coupled receptor protein signaling pathway' gene set. They span a plethora of overlapping GPCR-related genes that include GABAergic receptors (GABBR2, GABBR1, GABRA2, GABRE, GABRA4, GABRG2, GABRB2, GABRA1, GABRA3), cholinergic receptors (CRHR2, CHRM3), glutamatergic receptors (GRM5, GRM8, GRM2), adrenergic receptors (ADRA1B, ADRA2A), opioid receptors (OPRM1, OPRK1, OPRL1), neuropeptide Y receptors (NPY1R, NPY5R), and one dopamine receptor (DRD1). Also, 2 of the top 15 gene sets downregulated involve neuropeptide activity ('neuropeptide binding' and 'neuropeptide receptor activity'). Genes specifically impacted include tachykinin receptors (TACR2, TACR3), bombesin-like receptor 3 (BRS3), and somatostatin receptor 1 (SSTR1). In addition to many changes in receptor regulation, 'RNA binding' and 'structural constituent of ribosome' are negatively regulated along with 3 gene sets related to translation: 'translation initiation factor activity', 'translation factor activity nucleic acid binding', and 'translation' along with the final gene set 'cellular respiration' (ranked 15).

Cytoscape Pathway and Functional Enrichment Analyses

Out of the 710, 1,076, and 239 DEGs with nominal $p<0.05$ from differential analysis, Cytoscape generated networks with 672 nodes (2,450 edges), 1,000 nodes (5,254 edges), and 226 nodes (543 edges) for PND35 EtOH vs H_2O, PND46 EtOH vs H_2O, PND70 EtOH vs H_2O, respectively, where the number of nodes correspond to the genes in each of the networks. Using

clusterMaker and StringApp within Cytoscape, 7, 10, and 4 subnetworks with cluster sizes of at least 10 nodes were identified where 2, 3, and 2 subnetworks met the criteria of having: (1) at least 15 nodes (i.e., enriched genes), (2) genes that belong to the top 15 enriched functions based on their presence in GO Processes, KEGG Pathways, or Reactome Pathways, and (3) genes involved in particular topics, such as remodeling, immune response, and synaptic/signaling for PND35 EtOH vs H_2O, PND46 EtOH vs H_2O, PND70 EtOH vs H_2O, respectively.

Cytoscape analyses for PND35 EtOH vs H_2O (24 hours after the 4th dose): Earliest timepoint

For PND35, the top 2 clusters (from 3 subnetworks with at least 15 nodes) met all criteria previously described. In *Cluster 1 (PND35)*, for the Reactome Pathways, the top enriched functions identified are 'adaptive immune system' (Figure 8), 'immune system' (Figure 9), 'VEGFA-VEGFR2 pathway', and 'class I MHC mediated antigen processing and presentation', respectively. 'Antigen processing: ubiquitination & proteasome degradation' was the 6th most significant function under Reactome Pathways. Interestingly, other functions included genes that are also associated with neurodevelopmental processes. These include 'RHO GTPase Effectors' (Figure 10), 'Signaling by NOTCH' (Figure 11), 'Axon guidance', 'Integrin αIIb β3 signaling' (Figure 12), 'Developmental Biology', and 'L1CAM interactions'. For the GO Processes, the functions enriched vary greatly, from 'cellular response to hormone stimulus' (1 of 15), 'regulation of anatomical structure morphogenesis' (5 of 15), to 'positive regulation of phosphorylation' (11 of 15). For in KEGG pathways, 10 of the top 15 enriched gene sets include genes involved in cancer pathways, where the top two are 'breast cancer' and 'glioma',

respectively, but also include pancreatic, colorectal, and prostate cancer pathways indicative of cellular remodeling. Cellular senescence is 3rd in the top 15 enriched gene sets.

In *Cluster 2 (PND35)*, Reactome Pathways' GPCR ligand binding (1 of 15) and all 15 of the top enriched functions involve G-proteins. For GO Processes, the top significantly enriched pathway is 'G protein-coupled receptor signaling pathway' all other enriched pathways involve cell signaling and cellular response to stimulus. KEGG Pathways involve serotonergic (1 of 15), endocannabionoid (2 of 15), cholinergic (3 of 15), GABAergic (4 of 15), glutamatergic (7 of 15), and dopaminergic pathways (8 of 15). Other functions of interest include 'circadian entrainment' (5 of 15), 'chemokine signaling pathway' (6 of 15) (Figure 13), morphine addiction (10 of 15), and alcoholism (12 of 15).

Cytoscape analyses for PND46 EtOH vs H_2O (24 hours after the last dose; 10th dose)

For PND46, the top 3 clusters (from 5 subnetworks with at least 15 nodes) met all criteria. In *Cluster 1 (PND46)*, for the Reactome Pathways, 'immune system' (1 of 15) and 'innate immune system' (3 of 15) (Figures 14 and 15) had the highest number of enriched genes in this cluster (36 and 21, respectively). Genes encoding for Rho GTPases were also significantly enriched in 4 of the top 15 functions (Signaling by Rho GTPases' (Figure 16), 'RHO GTPases Activate WASPs and WAVEs', 'Rho GTPase cycle', and 'RHO GTPase Effectors') while 3 of the top 15 functions were involved in cell death pathways, namely: 'Regulation of actin dynamics for phagocytic cup formation', 'Class I MHC mediated antigen processing & presentation', and 'Antigen processing: Ubiquitination & Proteasome degradation'. GO Processes showed enrichment of functions involved in 'cell differentiation' (1 of 15) and immune activation ('immune system process' (2 of 15) (Figure 17) and 'cellular response to cytokine stimulus' (10

of 15)) (Figure 18). Other functions involved neurodevelopment, neuronal and synaptic remodeling genes ('regulation of cytoskeleton organization' (5 of 15) (Figure 19), 'regulation of plasma membrane bounded cell projection organization' (6 of 15), 'regulation of protein polymerization' (7 of 15), 'positive regulation of actin filament polymerization' (12 of 15), 'regulation of dendrite development' (14 of 15) (Figure 20), and 'neurogenesis' (15 of 15)). KEGG Pathways also demonstrate enrichment of functions involved in neuronal and synaptic development and remodeling (regulation of actin cytoskeleton (1 of 15) (Figure 21), focal adhesion (4 of 15), adherens junction (8 of 15), and axon guidance (10 of 15)). 2 functions associated with neuroimmune and cell death pathways are enriched (Fc gamma R-mediated phagocytosis (3 of 15) and T cell receptor signaling pathway (5 of 15)) (Figure 22).

In *Cluster 2 (PND46)*, Reactome Pathways are dominated by remodeling pathways that account for 10 of the top 15 enriched functions ('extracellular matrix organization' (1 of 15) (Figure 23), 'collagen formation' (2 of 15), 'collagen biosynthesis and modifying enzymes' (3 of 15), 'assembly of collagen fibrils and other multimeric structures' (5 of 15), 'degradation of the extracellular matrix' (6 of 15), 'laminin interactions' (7 of 15) (Figure 24), 'collagen chain trimerization' (10 of 15), 'elastic fibre formation' (12 of 15), 'integrin cell surface interactions' (13 of 15) (Figure 25), and 'collagen degradation' (14 of 15). For the GO Processes, pathways contain a high number of remodeling pathways, including 'response to stress' (2 of 15) (Figure 26), 'response to wounding' (3 of 15), 'wound healing' (5 of 15), 'regulation of cell migration' (6 of 15), 'positive regulation of biological process' (7 of 15), and 'positive regulation of cellular process' (15 of 15). KEGG Pathways also contain a number of remodeling pathways ('focal adhesion' (3 of 15), 'ECM-receptor interaction' (6 of 15) (Figure 27), 'Ras signaling pathway' (14 of 15) and neuroimmune pathways ('PI3K-Akt signaling pathway' (1 of 15) (Figure 28),

'cytokine-cytokine receptor interaction' (11 of 15) (Figure 29), and 'AGE-RAGE signaling pathway in diabetic complications' (15 of 15)).

In *Cluster 3 (PND46)*, G protein signaling and ligand binding events represent the top 4 of 15 enriched Reactome Pathways. Genes involved in Ca^{2+} signaling are also enriched ('Ca^{2+} pathway' (8 of 15)). 'G protein-coupled receptor signaling pathway' also represents the most significantly enriched gene pathway within the GO Processes with 'cellular Ca^{2+} ion homeostasis' (12 of 15) also showing enrichment. Six other groups involved in cell-cell communication and response to stimulus are enriched (signal transduction' (2 of 15), response to stimulus' (3 of 15), 'cellular response to stimulus' (4 of 15), 'regulation of cell communication' (10 of 15), 'regulation of signaling' (11 of 15), and 'positive regulation of signal transduction' (14 of 15)). Related to cell communication, KEGG Pathways demonstrate enrichment of multiple classes of neurons that include 5HT (1 of 15), ACh (6 of 15), Glut (7 of 15), DA (8 of 15), and GABA (11 of 15). Once again as seen at the previous time point (PND35), 'circadian entrainment' (4 of 15) is enriched along with 'morphine addiction' (5 of 15), 'alcoholism' (14 of 15), and 'chemokine signaling pathway' (12 of 15) (Figure 30).

Cytoscape analyses for PND70 EtOH vs H_2O (26 days after the last dose)

For PND70, the top 2 clusters (from 3 subnetworks with at least 15 nodes) met all criteria. In *Cluster 1 (PND70)*, the Reactome Pathways and GO Processes top gene sets were dominated by pathways involved in metabolic processes. For the Reactome Pathways, the enriched functions include 'the citric acid (TCA) cycle and respiratory electron transport' (1of 5), 'respiratory electron transport, ATP synthesis by chemiosmotic coupling, and heat production' (2 of 5), 'complex I biogenesis' (3 of 5), 'formation of ATP by chemiosmotic coupling' (4 of 5), and

'cristae formation' (5 of 5). For the GO processes, all top 15 enriched pathways involved metabolic processes with the top 3 being 'electron transport chain' (1 of 15), 'respiratory electron transport chain' (2 of 15), and 'cellular respiration' (3 of 15). For the KEGG Pathways, metabolic pathways accounted for 3 of the top 9 enriched pathways ('oxidative phosphorylation' (1 of 9), 'thermogenesis' (3 of 9), and 'metabolic pathways' (6 of 9)). Degenerative disease gene sets account for another 3 top enriched pathways ('Parkinson's disease' (2 of 9), 'Alzheimer's disease' (4 of 9), and 'Huntington's disease' (5 of 9)). 'Non-alcoholic fatty liver disease (NAFLD)' (7 of 9), 'retrograde endocannabinoid signaling' (8 of 9), and 'cardiac muscle contraction' (9 of 9) represent the final 3 enriched pathways within the KEGG Pathways at this time point.

In *Cluster 2 (PND70)*, only 1 Reactome Pathways gene set had a significant FDR value (0.029), which was the 'AKT phosphorylates targets in the nucleus' but only two genes were enriched (Akt1 and Foxo4). For the GO Processes, 6 of the top 15 enriched functions were related to cellular response, where the top 2 included 'response to endogenous stimulus' (1 of 15) and 'cellular response to endogenous stimulus' (2 of 15). 5 of the top 15 enriched functions were involved in negative regulation of 'negative regulation of cellular process' (3 of 15), 'negative regulation of signal transduction' (6 of 15), 'negative regulation of cellular macromolecule biosynthetic process' (8 of 15), 'negative regulation of macromolecule metabolic process' (14 of 15), and 'negative regulation of gene expression' (15 of 15). The KEGG Pathways showed enrichment of 5 cancer pathways ('breast cancer' (1 of 15), 'proteoglycans in cancer' (3 of 15), 'pathways in cancer' (5 of 15), 'gastric cancer' (13 of 15), 'hepatocellular carcinoma' (14 of 15), and enrichment of 'p53 signaling pathway' (4 of 15). Cellular apoptosis gene sets were enriched

in 3 pathways ('FoxO signaling pathway' (7 of 15), 'apoptosis' (8 of 15), and 'mTOR signaling pathway' (12 of 15) (Figure 31).

DISCUSSION

Differential Expression Analysis

Among the three timepoints, only the earliest timepoint (PND35) had 12 DEGs with FDR≤0.05, which allowed generation of a heatmap. The latter timepoints (PND46 and PND70) only had 1 DEG each, which are Wfs1 and Klra2, respectively. At the earliest timepoint only 2 genes stood out, period circadian regulator 3 (Per3) and cadherin 9 (Cdh9). Per3 is important because, as suggested by the name, it is involved in the regulation of circadian rhythm and higher homeostatic sleep drive (Dijk & Archer, 2010). Dysregulation of Per3 is important because 36-72% of patients with AUD report sleep disturbances that usually occur in the form of insomnia and that can persist into sobriety (Brower, 2003). Severity of sleep disturbance is suggested to correlate with likelihood of relapse (Brower et al., 2001). Another gene of interest is Cdh9, shown to selectively regulate synapse development between dentate gyrus (DG) and CA3 neurons within the hippocampus (Williams et al., 2011). Dysregulation of Cdh9 results in disruption of DG-CA3 synapse formation. Whether changes in Cdh9 also contribute to ectopic hippocampal neurogenesis (McClain et al., 2014) or subsequent changes in neuronal connectivity within the DG-CA3 region is yet to be determined but may be important in the context of spatial learning and memory processes.

Pathway-based Enrichment Analyses for Candidate Gene Identification

GSEA

Neuronal and Synaptic Remodeling

At the 4th dose (PND35), 5 of the top 15 gene sets downregulated were associated with the extracellular matrix. Gene families strongly regulated included laminins, collagens, thrombospondin4, and tenascin XB. One gene that stood out was FXR1, which is associated with mental retardation and is characterized by abnormal increased density of dendritic spines and the persistence of an immature dendritic spine phenotype. This is interesting since previous work in CA1 hippocampus has demonstrated the persistence of immature dendritic spines into adulthood following AIE (Risher et al., 2015a) suggesting a possible role for this gene in the dysregulation of dendritic spine development following AIE. By 24 hours after the 10th dose (PND46), 8 of the top 15 gene sets negatively regulated included genes associated with the extracellular matrix demonstrating continued negative regulation of many proteins involved in neuronal remodeling. Interestingly, there was a subset of genes that were specifically involved in axonogenesis, neurogenesis, and neuronal differentiation that were upregulated. A few other genes of importance were homer homolog 1 (HOMER1) and HOMER2 and neuroligin 1 (NLGN1). In thalamocortical synapses astrocyte secreted hevin was demonstrated to play a pivotal role in bridging neurexin-1α and neuroligin-1β for the assembly of glutamatergic synapses (Stogsdill et al., 2017). More recently, neuroligins were shown to play a role in regulating astrocyte complexity and morphogenesis (Stogsdill et al., 2017). HOMER1 has been shown to contribute to the regulation of Ca^{2+} dynamics in normal and reactive astrocytes (Buscemi et al., 2017). They have also been shown to regulate Ca^{2+} homeostasis at synaptic dendritic spines (Sala et al., 2005). These data may suggest that while key genes necessary for neuronal remodeling are

negatively regulated during AIE, select genes involved in synaptogenesis are starting to show enrichment. This is reflected by previous work in which increased synaptogenesis at the 10th dose time point (PND46) has been reported (Risher et al., 2015b). By PND70, 9 out of the top 15 enriched gene sets are related to neuronal and synaptic remodeling. Of particular interest are the genes that regulate neuropilin 1, CamKII, ephrin A4, and EPH receptor B2. Neuropilin 1 is involved in cell migration. Interestingly, ectopic hippocampal adult neurogenesis following adolescent alcohol exposure has been reported following repeated ethanol exposure (McClain et al., 2014). Given the role that neuropilin 1 plays in cell migration, disruption of this gene regulation may contribute to the development of aberrant adult neurogenesis (McClain et al., 2014). CaM kinase II is involved in many functions including dendritic spine development (Cornelia Koeberle et al., 2017). Ephrins are most commonly associated with synaptic development and synaptic remodeling. Ephrin A4 mimetics that target the EphA receptor impair the formation of long-term fear memory (Dines & Lamprecht, 2014). While EphB2 has been associated with stress vulnerability and the modulation of fear extinction in adolescent rats (Cruz et al., 2015; Zhang et al., 2016). Combined with the enrichment of numerous ECM-related proteins involved in neuronal remodeling these data suggest that there is heightened plasticity that could result in the development of aberrant circuitry specifically associated with memory processes within the CA1 that persists into adulthood.

Neuroinflammation

At PND35 (24 hours after the 4th dose), none of the gene sets within the top 15 enriched or negatively regulated included genes involved in neuroinflammation. By PND46 (24 hour after the 10th dose), there were indications of a reduction in neuroinflammation gene activation as

demonstrated by negative regulation of C1q and IL1β. These are two of the three proteins necessary for microglia induced A1 astrocyte activation (the other being TNFα). A1 astrocyte activation results in a loss of neuronal support and induction of neurotoxicity that can result in neuronal death. Negative regulation of these two genes only occurring at PND46 (24 hours after the 10th dose) and not at PND35 (24 hours after the 4th dose) would suggest that M1 microglial activation does not take place immediately following AIE and that repeated ethanol exposure may be critical for inducing glial activation at this particular dose of ethanol. Lack of microglial induced reactivity is supported by the downregulation of the gene that encodes the lipopolysaccharide binding protein (LBP) which is typically upregulated via the M1 activation pathway. Further evidence that glial reactivity pathways are downregulated comes from the negative regulation of Kallikrein-6 (KLK6). Kallikrein-6 upregulation contributes to astrocyte reactivity (Scarisbrick et al., 2012), and is suggested to modulate astrocyte morphogenesis via proteinase activated receptors (PARs) (Yoon et al., 2018). In addition to negative regulation of select neuroimmune genes there is also negative regulation of the genes involved in neuronal death cascades. Loss of genes that encode for neuronal death processes may explain the proliferative burst of adult neurogenesis that has been observed in the dentate gyrus following repeated ethanol exposure (Hayes et al., 2018) that is then followed by delayed adult newborn neuron cell loss (Liu & Crews, 2017).

By 26 days after the last dose (PND70), neuroinflammatory genes previously negatively regulated have recovered to baseline levels. However, a select few important genes and gene sets involved in regulating neuroinflammatory cascades are enriched. These include the single immunoglobulin and toll-interleukin 1 receptor (TIR) domain (SIGIRR). The phylogenetically conserved Toll/IL-1 receptor (TIR) domain plays a central role in Toll-like receptor (TLR)

signaling by recruiting adaptor proteins such as MyD88, Mal, TRIP, and TRAM. It is also involved in the activation of transcription factors that regulate proinflammatory cytokines such as, IL-1, IL-6, IL-8 and TNF-α (Narayanan & Park, 2015). Receptor (TNFRSF)-interacting serine-threonine kinase 1 (RIPK1), tumor necrosis factor superfamily, member 1A, 10, and 10B (TNFRSF1A, TNFRSF10 and TNFRSF10B), lipopolysaccharide-induced TNF factor (LITAF), caspase 8 (CASP8), Ras homolog gene family member A and C (RHOA and RHOC), and mindbomb homolog 2 (MIB2) were all enriched and are all involved in neuroinflammation and/or cell death pathways. LITAF encodes a DNA-binding protein that mediates TNFα expression (Myokai et al., 1999). The TNFRSF gene family itself is involved in the regulation of neuroinflammation and induction of apoptosis through the activation of caspase 8 (Wang et al., 2008) while RIPK1, a gene that encodes a member of the receptor-interacting protein (RIP) family of serine/threonine protein kinases, is involved in regulating neuroinflammation and cell death through apoptotic and necrotopic pathways (Lalaoui et al., 2020; Weinlich & Green, 2014). Together these data suggest that the protracted upregulation of neuroinflammatory genes could contribute to the presence of chronic neuroinflammation and induction of astrocyte reactivity that has previously been described in a rat model of adolescent binge drinking (Liu et al., 2020; Risher et al., 2015b).

Addiction

Tachykinin receptors (TACR2, TACR3) encode for tachykinin neuropeptide substance K (NK2 and NK3). Huang et al. (2018) showed that low-anxiety mice have a greater preference for ethanol when compared to the high-anxiety mouse group. Low-anxiety mice also had higher levels of NK1 receptor (NKR1) in the hippocampus when compared to the high-anxiety group.

In addition, Ribeiro and De Lima (2002) demonstrated that NKR2 antagonists can block the anxiogenic effects of pentylenetetrazol. Combined, these data may suggest a role for NKRs in anxiety and alcohol reward in adolescent mice (Huang et al., 2018) that may also be important in this rat model of adolescent binge drinking.

Receptor Function

At PND35 (24 hour after the 4th dose), there was select downregulation of a number of genes encoding for glutamate receptors (GRIK2/GluR6, GRIK1/GluR5, GRM8/mGluR8), dopaminergic receptors (DRD1 and DRD4), and the adenosine A2a receptor (ADORA2A). At PND46 (24 hour after the 10th dose), genes encoding for GluR5 and GluR6 became enriched along with protracted enrichment of genes encoding for GluN2A, GluN2B, GluA2, GluR7, GluA1, mGluR5, mGluR3, and mGluR7. By PND70, gene expression returned to normal baseline levels or were negatively regulated. Genes encoding for mGluR5, mGluR8, and DRD1 were upregulated at PND46 but by PND70 were significantly downregulated. These are important changes since mGluR5 receptors are found on astrocytes and are important for maintaining glutamate homeostasis within the synaptic cleft. Changes in receptor expression could profoundly impact the clearance of glutamate by astrocytes and therefore influence neuronal excitability. The dopamine receptor D1 (DRD1) is involved in the reward pathway and is heavily involved in substance and alcohol use disorder emergence and relapse. Most recently, D1R-expressing neurons within the DG have been implicated in the extinction of cocaine-associated contextual memories (Burgdorf et al., 2020) suggesting that downregulation of DRD1 may play a role in the permanence of reward-associated memories.

Most impacted through negative regulation were genes encoding for cholinergic receptors CHRNA7/nACh7, CHRM3/M3, CHRNA5/nACh5, CHRNA4/nACh4, CHRNE and the GABAergic receptors GABBR2/GABA-BR2, GABBR1/GABA-BR1, GABRA2/GABA-A2, GABRE/GABA-E, GABRA4/GABA-A4, GABRG2/GABA-AG2, GABRB2/GABA-B2, GABRA1/GABA-A1, GABRA3/GABA-A3. Negative regulation of cholinergic receptors occurs in parallel to a loss of cholinergic neurons that has been reported in the basal forebrain following AIE (Fernandez & Savage, 2017; Vetreno & Crews, 2018) suggesting that AIE results in cholinergic neuronal loss and prolonged dysregulation that could be critical for modulation of neuronal circuitry and learning and memory processes. Negative regulation of numerous genes that encode for GABAergic receptors, while many genes encoding for glutamatergic receptors remain at control levels or are downregulated, bolsters the previously proposed hypothesis that AIE results in dysregulation of inhibitory:excitatory balance (Spear & Swartzwelder, 2014a) with a shift towards less inhibition, driving increased excitation. Increased excitation or reduced inhibition has been demonstrated in a number of studies that show lowered threshold for LTP in CA1 (Risher et al., 2015a), reduction in tonic inhibition in dentate gyrus (Fleming et al., 2011), and changes in interneuron firing rate in inhibitory interneurons of the CA1 (Yan et al., 2009).

Potassium Channels

At PND35 (24 hours after the 4th dose), genes encoding for ion channel activity were selectively enriched for a subset of potassium ions (KCNAB2, KCNV1, KCNAB3, KCNS3, KCNAB1), while others were downregulated (KCNMA1, KCNK5, KCNQ3, KCNK3, KCNQ4). At PND46 (24 hours after the 10th dose), there was a rebound in K^+ channel genes (26 of 50 genes were enriched) suggesting unique profiles of K^+ channel gene regulation that are dependent on the

duration of ethanol exposure. Three genes in particular transitioned from negative regulation to positive regulation across the dosing paradigm, they include: KCNMA1 (KCa1.1), KCNQ3 (Kv7.3), KCNC4 (Kv3.4). Enrichment of these genes, combined with enrichment of other genes such as KCNJ10 that encodes for Kir4.1, an astrocyte K+ channel that is involved in ion homeostasis of the synaptic cleft during neuronal activity could suggest that there is a compensatory increase in K+ channel expression in an attempt to dampen neuronal excitability following AIE. Interestingly, by PND70, following the washout period, K^+ channel activity is again negatively regulated. This is reflected in 2 of the top 15 gene sets. KCNMA1 (KCa1.1) and KCNC4 (Kv3.4) once again received opposing regulation at this later time point along with KCNH2 (Kv11.1), KCNA3 (Kv1.3), KCNH4 (Kv12.3), and KCNH3 (Kv12.2). Kv channels are voltage dependent K^+ channels that play an important role in regulating neuronal excitability and stabilizing the membrane potential. KCNMA1 (KCa1.1) channels are activated by membrane depolarization and increased cytosolic Ca^{2+} and contribute to membrane repolarization thus contributing to the regulation of neuronal excitability. KCNC4 (Kv3.4) channels are delayed rectifiers that mediate voltage-dependent potassium ion permeability of excitable membranes. The KCNH2 (Kv11.1) is a pore forming (α) subunit of the voltage-gated inwardly rectifying potassium channel. KCNA3 (Kv1.3) channels. KCNH4 (Kv12.3) is another pore forming subunit of the voltage-gated K+ channel, whereas KCNH3 (Kv12.2) is an important regulator of excitability in hippocampal pyramidal cells. Genetic deletion and/or pharmacological blockade of this K^+ channel in mice has been shown to result in neuronal hyperexcitability that include the emergence of spontaneous seizures (Zhang et al., 2010). While it is common knowledge that K^+ channels play a critical role in the regulation and homeostasis of neuronal excitability, little work

has been conducted to explore their role in the development of neuronal excitability in the hippocampus following AIE.

Cytoscape Pathway and Functional Enrichment Analyses

The stringent yet a bit permissive cut-off ($p<0.05$) used allowed us to capture the stronger signals (i.e., a subset) in terms of functional enrichment. Use of a higher cut-off may allow inclusion of other functions, such as the K+ channels as discussed below.

Neuronal and Synaptic Remodeling

At PND35 (24 hours after the 4th dose), 'RHO GTPase effectors', 'signaling by NOTCH', 'axon guidance', 'Integrin αIIb β3 signaling', 'Developmental Biology', 'L1CAM interactions', 'regulation of anatomical structure morphogenesis', and 'anatomical structure morphogenesis' are enriched. While the list of effected pathways remains small at this timepoint, it may indicate that enrichment of neuronal and synaptic remodeling is beginning. At PND46 (24 hours after the 10th dose), 'signaling by Rho GTPases', 'RHO GTPases Activate WASPs and WAVEs', 'Rho GTPase cycle', and 'RHO GTPase Effectors' were enriched but all enrichment returned to age-matched controls by PND70. These changes at PND46 (24 hours after the 10th dose) appear to be associated with cytoskeletal reorganization as indicated by enrichment of at least 18 individual pathways that are associated with these processes. While many genes are enriched there are two that are particularly interesting, i.e. RHOA and Rac1, which are involved in the regulation of dendritic branch complexity and spine morphology (Nakayama et al., 2000). Moreover specifically, Rac1 has been implicated in thrombospondin-induced synaptogenesis (Risher et al., 2018). And, previous work has demonstrated that astrocyte secreted

thrombospondins are upregulated following AIE at this timepoint at the protein level. This coincided with an increase in synaptogenesis (Risher et al., 2015b). Whether these new synapses represent aberrant synaptogenesis that could contribute to the strengthening of memory circuits associated with reward is yet to be determined. In addition to enrichment of pathways that involve cytoskeletal and extracellular matrix organization, pathways involved in wound healing were also enriched. These changes could be indicative of the release of signaling factors involved in remodeling in an attempt to restore damaged circuitry after insult.

Neuroinflammation

Contrary to the gene expression analysis in which there was no enrichment or negative regulation of neuroinflammatory genes, at PND35 (24 hours after the 4th dose), adaptive and innate neuroimmune pathway activation were enriched using pathway analysis. Enriched pathways included chemokine-related pathways, antigen presentation and processing, and apoptotic processes. At PND46 (24 hours after the 10th dose), the number of enriched pathways associated with neuroimmune processes and cell death pathways (including phagocytosis) were increased. New pathways included 'cytokine-cytokine receptor interaction' and 'AGE-RAGE signaling pathway in diabetic complications'. The majority of genes within these pathways do not have exclusive functions only within neuroinflammatory cascades, however some functions converge upon these inflammatory pathways. Some of the more interesting genes activate the JAK-STAT pathway, these include IFNAR1, IL6, and CRLF2. The JAK-STAT pathway is important because it is involved in a variety of signaling processes that can stimulate cell proliferation, differentiation, and apoptosis, and plays a pivotal role in immune processes (Rawlings et al., 2004). Most recently, it has been suggested to play a role in astrocyte reactivity (Park et al.,

2003; Van Wagoner & Benveniste, 1999) Another indication that astrocyte reactivity could be occurring is due to the enrichment of IL1R1 which encodes for IL-1α and IL-1β one of the activators of A1 astrocyte reactivity. However, by PND70, all enriched pathways associated with neuroinflammatory processes returned to baseline in the pathway analysis despite upregulation of key select genes in the GSEA that are typically associated with neuroinflammatory processes (THBS4, JAK2, numerous TNFR subtypes, SIGIRR, LITAF, CASP8, and RIPK1).

Addiction

At PND35 (24 hours after the 4th dose), pathways associated with morphine addiction and alcoholism were enriched. Enrichment of these pathways coincided with activation of neuroimmune pathways and enrichment of pathways involved in neuronal and synaptic remodeling. At PND46 (24 hours after the 10th dose), these two addiction-related pathways remained enriched ('morphine addiction' and 'alcoholism') and consisted mainly of G Protein subunits.

Receptor Function

At PND35 (24 hours after the 4th dose), many of the enriched pathways involved neuronal subtypes that include 5HT, endocannabionoid, ACh, GABA, Glut, and DA pathways. This is somewhat consistent with GSEA results in which Glut and DA receptors were enriched at this early timepoint. At PND46 (24 hour after the 10th dose), enrichment of multiple classes of neurons persisted (5HT, ACh, Glut, DA, GABA) but by PND70, functional enrichment returned to age-matched control levels.

Potassium Channels

In the GSEA involving GO terms, select K^+ channel enrichment was beginning to emerge at PND35 (24 hours after the 4th dose). By 24 hours after the 10th dose (PND46), K^+ enrichment was highly prominent but became negatively regulated by PND70. This was not reflected in the Cytoscape pathway analysis in which K^+ channels did not reach the top pathways impacted by AIE at any timepoint.

FUNDING

This work was supported by the National Institutes of Health P20GM103434 [WV-INBRE grant (DAP, JD, and AQN), Veteran Affairs Career Development Award 1lK2BX002505 (M-LR), and NARSAD Young Investigator Award 25432 (M-LR).

CONCLUSION

GSEA and Cytoscape pathway and enrichment analyses, in which whole dataset and subset ($p<0.05$) were used as input, respectively, provide detailed insight into how hippocampal gene expression changes across adolescence and into adulthood (Figure 32). Our findings also provide a comprehensive screening of the acute and long-term effects of adolescent ethanol exposure on gene expression. Some of the findings presented here support our previous work demonstrating long-term upregulation of proteins that are involved neuronal remodeling. These data also uncover novel pathways that will be an invaluable guide to understanding the mechanisms underlying the acute and long-term effects of adolescent ethanol exposure.

REFERENCES

Acheson, S. K., Bearison, C., Risher, M. L., Abdelwahab, S. H., Wilson, W. A., & Swartzwelder, H. S. (2013). Effects of acute or chronic ethanol exposure during adolescence on behavioral inhibition and efficiency in a modified water maze task. *PLoS One, 8*(10), e77768. doi:10.1371/journal.pone.0077768

Anders, S., Pyl, P. T., & Huber, W. (2015). HTSeq--a Python framework to work with high-throughput sequencing data. *Bioinformatics, 31*(2), 166-169. doi:10.1093/bioinformatics/btu638

Andrews, S. (2010). FASTQC. A quality control tool for high throughput sequence data. In.

Ashburner, M., Ball, C. A., Blake, J. A., Botstein, D., Butler, H., Cherry, J. M., . . . Sherlock, G. (2000). Gene ontology: tool for the unification of biology. The Gene Ontology Consortium. *Nat Genet, 25*(1), 25-29. doi:10.1038/75556

Benjamini, Y., & Hochberg, Y. (1995). Controlling the False Discovery Rate - a Practical and Powerful Approach to Multiple Testing. *Journal of the Royal Statistical Society, Series B, 57*(1), 289-300.

Brower, K. J. (2003). Insomnia, alcoholism and relapse. *Sleep Med Rev, 7*(6), 523-539. doi:10.1016/s1087-0792(03)90005-0

Brower, K. J., Aldrich, M. S., Robinson, E. A., Zucker, R. A., & Greden, J. F. (2001). Insomnia, self-medication, and relapse to alcoholism. *Am J Psychiatry, 158*(3), 399-404. doi:10.1176/appi.ajp.158.3.399

Burgdorf, C. E., Bavley, C. C., Fischer, D. K., Walsh, A. P., Martinez-Rivera, A., Hackett, J. E., . . . Rajadhyaksha, A. M. (2020). Contribution of D1R-expressing neurons of the dorsal dentate gyrus and Ca(v)1.2 channels in extinction of cocaine conditioned place preference. *Neuropsychopharmacology, 45*(9), 1506-1517. doi:10.1038/s41386-019-0597-z

Buscemi, L., Ginet, V., Lopatar, J., Montana, V., Pucci, L., Spagnuolo, P., . . . Bezzi, P. (2017). Homer1 Scaffold Proteins Govern Ca2+ Dynamics in Normal and Reactive Astrocytes. *Cereb Cortex, 27*(3), 2365-2384. doi:10.1093/cercor/bhw078

Centers for Disease Control and Prevention. (2019). *Alcohol Related Disease Impact (ARDI) application*. Retrieved from https://nccd.cdc.gov/DPH_ARDI

Chin, V., Van Skike, C., & Matthews, D. (2010). Effects of ethanol on hippocampal function during adolescence: a look at the past and thoughts on the future. *Alcohol, 44*(1), 3-14. doi:10.1016/j.alcohol.2009.10.015

Coleman, L. G., Jr., Liu, W., Oguz, I., Styner, M., & Crews, F. T. (2014). Adolescent binge ethanol treatment alters adult brain regional volumes, cortical extracellular matrix protein and behavioral flexibility. *Pharmacol Biochem Behav, 116*, 142-151. doi:10.1016/j.pbb.2013.11.021

Cornelia Koeberle, S., Tanaka, S., Kuriu, T., Iwasaki, H., Koeberle, A., Schulz, A., . . . Okabe, S. (2017). Developmental stage-dependent regulation of spine formation by calcium-calmodulin-dependent protein kinase IIalpha and Rap1. *Sci Rep, 7*(1), 13409. doi:10.1038/s41598-017-13728-y

Crews, F. T., Robinson, D. L., Chandler, L. J., Ehlers, C. L., Mulholland, P. J., Pandey, S. C., . . . Vetreno, R. P. (2019). Mechanisms of Persistent Neurobiological Changes Following Adolescent Alcohol Exposure: NADIA Consortium Findings. *Alcohol Clin Exp Res, 43*(9), 1806-1822. doi:10.1111/acer.14154

Cruz, E., Soler-Cedeño, O., Negrón, G., Criado-Marrero, M., Chompré, G., & Porter, J. T. (2015). Infralimbic EphB2 Modulates Fear Extinction in Adolescent Rats. *J Neurosci, 35*(36), 12394-12403. doi:10.1523/jneurosci.4254-14.2015

DeWit, D., Adlaf, E., Offord, D., & Ogborne, A. (2000). Age at first alcohol use: a risk factor for the development of alcohol disorders. *The American journal of psychiatry, 157*(5), 745-750.

Dijk, D. J., & Archer, S. N. (2010). PERIOD3, circadian phenotypes, and sleep homeostasis. *Sleep Med Rev, 14*(3), 151-160. doi:10.1016/j.smrv.2009.07.002

Dines, M., & Lamprecht, R. (2014). EphrinA4 mimetic peptide targeted to EphA binding site impairs the formation of long-term fear memory in lateral amygdala. *Transl Psychiatry, 4*(9), e450. doi:10.1038/tp.2014.76

Dobin, A., Davis, C. A., Schlesinger, F., Drenkow, J., Zaleski, C., Jha, S., . . . Gingeras, T. R. (2013). STAR: ultrafast universal RNA-seq aligner. *Bioinformatics, 29*(1), 15-21. doi:10.1093/bioinformatics/bts635

Doncheva, N. T., Morris, J. H., Gorodkin, J., & Jensen, L. J. (2019). Cytoscape StringApp: Network Analysis and Visualization of Proteomics Data. *J Proteome Res, 18*(2), 623-632. doi:10.1021/acs.jproteome.8b00702

Fernandez, G. M., & Savage, L. M. (2017). Adolescent binge ethanol exposure alters specific forebrain cholinergic cell populations and leads to selective functional deficits in the prefrontal cortex. *Neuroscience, 361*, 129-143. doi:10.1016/j.neuroscience.2017.08.013

Fleming, R. L., Acheson, S. K., Moore, S. D., Wilson, W. A., & Swartzwelder, H. S. (2011). GABA transport modulates the ethanol sensitivity of tonic inhibition in the rat dentate gyrus. *Alcohol (Fayetteville, N.Y.), 45*(6), 577-583. doi:10.1016/j.alcohol.2011.03.003

Fox, M. E., Chandra, R., Menken, M. S., Larkin, E. J., Nam, H., Engeln, M., . . . Lobo, M. K. (2020). Dendritic remodeling of D1 neurons by RhoA/Rho-kinase mediates depression-like behavior. *Mol Psychiatry, 25*(5), 1022-1034. doi:10.1038/s41380-018-0211-5

Fujii, S., Yamazaki, Y., Sugihara, T., & Wakabayashi, I. (2008). Acute and chronic ethanol exposure differentially affect induction of hippocampal LTP. *Brain Res, 1211*, 13-21. doi:10.1016/j.brainres.2008.02.052

Grant, B. F., & Dawson, D. A. (1997). Age at onset of alcohol use and its association with DSM-IV alcohol abuse and dependence: results from the National Longitudinal Alcohol Epidemiologic Survey. *J Subst Abuse, 9*, 103-110. doi:10.1016/s0899-3289(97)90009-2

Hanson, K., Medina, K., Padula, C., Tapert, S., & Brown, S. (2011). Impact of Adolescent Alcohol and Drug Use on Neuropsychological Functioning in Young Adulthood: 10-Year Outcomes. *Journal of child & adolescent substance abuse, 20*(2), 135-154. doi:10.1080/1067828x.2011.555272

Harper, C., & Matsumoto, I. (2005). Ethanol and brain damage. *Curr Opin Pharmacol, 5*(1), 73-78. doi:10.1016/j.coph.2004.06.011

Hasin, D. S., Stinson, F. S., Ogburn, E., & Grant, B. F. (2007). Prevalence, correlates, disability, and comorbidity of DSM-IV alcohol abuse and dependence in the United States: results from the National Epidemiologic Survey on Alcohol and Related Conditions. *Arch Gen Psychiatry, 64*(7), 830-842. doi:10.1001/archpsyc.64.7.830

Hayes, D. M., Nickell, C. G., Chen, K. Y., McClain, J. A., Heath, M. M., Deeny, M. A., & Nixon, K. (2018). Activation of neural stem cells from quiescence drives reactive hippocampal neurogenesis after alcohol dependence. *Neuropharmacology, 133*, 276-288. doi:10.1016/j.neuropharm.2018.01.032

Huang, H., Zhang, X., Fu, X., Zhang, X., Lang, B., Xiang, X., & Hao, W. (2018). Alcohol-induced conditioned place preference negatively correlates with anxiety-like behavior in adolescent mice: inhibition by a neurokinin-1 receptor antagonist. *Psychopharmacology (Berl), 235*(10), 2847-2857. doi:10.1007/s00213-018-4976-7

Huber, W., Carey, V. J., Gentleman, R., Anders, S., Carlson, M., Carvalho, B. S., . . . Morgan, M. (2015). Orchestrating high-throughput genomic analysis with Bioconductor. *Nat Methods, 12*(2), 115-121. doi:10.1038/nmeth.3252

Isherwood, S. N., Robbins, T. W., Dalley, J. W., & Pekcec, A. (2018). Bidirectional variation in glutamate efflux in the medial prefrontal cortex induced by selective positive and negative allosteric mGluR5 modulators. *J Neurochem, 145*(2), 111-124. doi:10.1111/jnc.14290

Jassal, B., Matthews, L., Viteri, G., Gong, C., Lorente, P., Fabregat, A., . . . D'Eustachio, P. (2020). The reactome pathway knowledgebase. *Nucleic Acids Res, 48*(D1), D498-D503. doi:10.1093/nar/gkz1031

Kanehisa, M. (2019). Toward understanding the origin and evolution of cellular organisms. *Protein Sci, 28*(11), 1947-1951. doi:10.1002/pro.3715

Kanehisa, M., & Goto, S. (2000). KEGG: kyoto encyclopedia of genes and genomes. *Nucleic Acids Res, 28*(1), 27-30. doi:10.1093/nar/28.1.27

Kanehisa, M., Sato, Y., Furumichi, M., Morishima, K., & Tanabe, M. (2019). New approach for understanding genome variations in KEGG. *Nucleic Acids Res, 47*(D1), D590-D595. doi:10.1093/nar/gky962

Kersey, P. J., Staines, D. M., Lawson, D., Kulesha, E., Derwent, P., Humphrey, J. C., . . . Birney, E. (2012). Ensembl Genomes: an integrative resource for genome-scale data from non-vertebrate species. *Nucleic Acids Res, 40*(Database issue), D91-97. doi:10.1093/nar/gkr895

Kim, E. U., Varlinskaya, E. I., Dannenhoffer, C. A., & Spear, L. P. (2019). Adolescent intermittent ethanol exposure: Effects on pubertal development, novelty seeking, and social interaction in adulthood. *Alcohol (Fayetteville, N.Y.), 75*, 19-29. doi:https://doi.org/10.1016/j.alcohol.2018.05.002

Krueger, F. (2020). TrimGalore (Version v0.6.6). Retrieved from https://github.com/FelixKrueger/TrimGalore

Kucheryavykh, Y. V., Kucheryavykh, L. Y., Nichols, C. G., Maldonado, H. M., Baksi, K., Reichenbach, A., . . . Eaton, M. J. (2007). Downregulation of Kir4.1 inward rectifying potassium channel subunits by RNAi impairs potassium transfer and glutamate uptake by cultured cortical astrocytes. *Glia, 55*(3), 274-281. doi:10.1002/glia.20455

Lalaoui, N., Boyden, S. E., Oda, H., Wood, G. M., Stone, D. L., Chau, D., . . . Silke, J. (2020). Mutations that prevent caspase cleavage of RIPK1 cause autoinflammatory disease. *Nature, 577*(7788), 103-108. doi:10.1038/s41586-019-1828-5

Liu, C. J., Chaturvedi, N., Barnstable, C. J., & Dreyer, E. B. (1996). Retinal Thy-1 expression during development. *Invest Ophthalmol Vis Sci, 37*(7), 1469-1473.

Liu, W., & Crews, F. T. (2017). Persistent Decreases in Adult Subventricular and Hippocampal Neurogenesis Following Adolescent Intermittent Ethanol Exposure. *Front Behav Neurosci, 11*, 151. doi:10.3389/fnbeh.2017.00151

Liu, W., Vetreno, R. P., & Crews, F. T. (2020). Hippocampal TNF-death receptors, caspase cell death cascades, and IL-8 in alcohol use disorder. *Mol Psychiatry*. doi:10.1038/s41380-020-0698-4

Love, M. I., Huber, W., & Anders, S. (2014). Moderated estimation of fold change and dispersion for RNA-seq data with DESeq2. *Genome Biol, 15*(12), 550. doi:10.1186/s13059-014-0550-8

Martin, M. (2011). Cutadapt removes adapter sequences from high-throughput sequencing reads. *2011, 17*(1), 3. doi:10.14806/ej.17.1.200

Matsunaga, E., Nambu, S., Oka, M., Tanaka, M., Taoka, M., & Iriki, A. (2015). Periostin, a neurite outgrowth-promoting factor, is expressed at high levels in the primate cerebral cortex. *Dev Growth Differ, 57*(3), 200-208. doi:10.1111/dgd.12194

McClain, J. A., Morris, S. A., Marshall, S. A., & Nixon, K. (2014). Ectopic hippocampal neurogenesis in adolescent male rats following alcohol dependence. *Addict Biol, 19*(4), 687-699. doi:10.1111/adb.12075

Mootha, V. K., Lindgren, C. M., Eriksson, K. F., Subramanian, A., Sihag, S., Lehar, J., . . . Groop, L. C. (2003). PGC-1alpha-responsive genes involved in oxidative phosphorylation are coordinately downregulated in human diabetes. *Nat Genet, 34*(3), 267-273. doi:10.1038/ng1180

Morris, J. H., Apeltsin, L., Newman, A. M., Baumbach, J., Wittkop, T., Su, G., . . . Ferrin, T. E. (2011). clusterMaker: a multi-algorithm clustering plugin for Cytoscape. *BMC Bioinformatics, 12*, 436. doi:10.1186/1471-2105-12-436

Myokai, F., Takashiba, S., Lebo, R., & Amar, S. (1999). A novel lipopolysaccharide-induced transcription factor regulating tumor necrosis factor alpha gene expression: molecular cloning, sequencing, characterization, and chromosomal assignment. *Proc Natl Acad Sci U S A, 96*(8), 4518-4523. doi:10.1073/pnas.96.8.4518

N'Gouemo, P. (2014). BKCa channel dysfunction in neurological diseases. *Front Physiol, 5*, 373. doi:10.3389/fphys.2014.00373

Nakayama, A. Y., Harms, M. B., & Luo, L. (2000). Small GTPases Rac and Rho in the Maintenance of Dendritic Spines and Branches in Hippocampal Pyramidal Neurons. *The Journal of Neuroscience, 20*(14), 5329-5338. doi:10.1523/jneurosci.20-14-05329.2000

Narayanan, K. B., & Park, H. H. (2015). Toll/interleukin-1 receptor (TIR) domain-mediated cellular signaling pathways. *Apoptosis, 20*(2), 196-209. doi:10.1007/s10495-014-1073-1

NIAAA. (2020). *Underage Drinking*. Retrieved from Bethesda, MD: https://www.niaaa.nih.gov/sites/default/files/Underage_Fact.pdf

Otasek, D., Morris, J. H., Boucas, J., Pico, A. R., & Demchak, B. (2019). Cytoscape Automation: empowering workflow-based network analysis. *Genome Biol, 20*(1), 185. doi:10.1186/s13059-019-1758-4

Pan, Y., Liu, G., Fang, M., Shen, L., Wang, L., Han, Y., . . . Wang, X. (2010). Abnormal expression of netrin-G2 in temporal lobe epilepsy neurons in humans and a rat model. *Exp Neurol, 224*(2), 340-346. doi:10.1016/j.expneurol.2010.04.001

Park, E. J., Park, S. Y., Joe, E. H., & Jou, I. (2003). 15d-PGJ2 and rosiglitazone suppress Janus kinase-STAT inflammatory signaling through induction of suppressor of cytokine signaling 1 (SOCS1) and SOCS3 in glia. *J Biol Chem, 278*(17), 14747-14752. doi:10.1074/jbc.M210819200

R Core Team. (2020). R: A Language and Environment for Statistical Computing. Vienna, Austria: R Foundation for Statistical Computing. Retrieved from https://www.R-project.org/

Rawlings, J. S., Rosler, K. M., & Harrison, D. A. (2004). The JAK/STAT signaling pathway. *J Cell Sci, 117*(Pt 8), 1281-1283. doi:10.1242/jcs.00963

Rehm, J. (2011). The risks associated with alcohol use and alcoholism. *Alcohol Res Health, 34*(2), 135-143.

Rehm, J., Anderson, P., Barry, J., Dimitrov, P., Elekes, Z., Feijao, F., . . . Gmel, G. (2015). Prevalence of and potential influencing factors for alcohol dependence in Europe. *Eur Addict Res, 21*(1), 6-18. doi:10.1159/000365284

Rehm, J., Mathers, C., Popova, S., Thavorncharoensap, M., Teerawattananon, Y., & Patra, J. (2009). Global burden of disease and injury and economic cost attributable to alcohol use and alcohol-use disorders. *Lancet, 373*(9682), 2223-2233. doi:10.1016/S0140-6736(09)60746-7

Ribeiro, R. L., & De Lima, T. C. (2002). Participation of GABAA receptors in the modulation of experimental anxiety by tachykinin agonists and antagonists in mice. *Prog Neuropsychopharmacol Biol Psychiatry, 26*(5), 861-869. doi:10.1016/s0278-5846(01)00331-1

Risher, M. L., Fleming, R. L., Boutros, N., Semenova, S., Wilson, W. A., Levin, E. D., . . . Acheson, S. K. (2013). Long-term effects of chronic intermittent ethanol exposure in adolescent and adult rats: radial-arm maze performance and operant food reinforced responding. *PLoS One, 8*(5), e62940. doi:10.1371/journal.pone.0062940

Risher, M. L., Fleming, R. L., Risher, W. C., Miller, K. M., Klein, R. C., Wills, T., . . . Swartzwelder, H. S. (2015a). Adolescent intermittent alcohol exposure: persistence of structural and functional hippocampal abnormalities into adulthood. *Alcohol Clin Exp Res, 39*(6), 989-997. doi:10.1111/acer.12725

Risher, M. L., Sexton, H. G., Risher, W. C., Wilson, W. A., Fleming, R. L., Madison, R. D., . . . Swartzwelder, H. S. (2015b). Adolescent Intermittent Alcohol Exposure: Dysregulation of Thrombospondins and Synapse Formation are Associated with Decreased Neuronal Density in the Adult Hippocampus. *Alcohol Clin Exp Res, 39*(12), 2403-2413. doi:10.1111/acer.12913

Risher, W. C., Kim, N., Koh, S., Choi, J. E., Mitev, P., Spence, E. F., . . . Eroglu, C. (2018). Thrombospondin receptor alpha2delta-1 promotes synaptogenesis and spinogenesis via postsynaptic Rac1. *J Cell Biol, 217*(10), 3747-3765. doi:10.1083/jcb.201802057

Sabeti, J., & Gruol, D. L. (2008). Emergence of NMDAR-independent long-term potentiation at hippocampal CA1 synapses following early adolescent exposure to chronic intermittent ethanol: role for sigma-receptors. *Hippocampus, 18*(2), 148-168. doi:10.1002/hipo.20379

Sacks, J. J., Gonzales, K. R., Bouchery, E. E., Tomedi, L. E., & Brewer, R. D. (2015). 2010 National and State Costs of Excessive Alcohol Consumption. *Am J Prev Med, 49*(5), e73-e79. doi:10.1016/j.amepre.2015.05.031

Sala, C., Roussignol, G., Meldolesi, J., & Fagni, L. (2005). Key role of the postsynaptic density scaffold proteins Shank and Homer in the functional architecture of Ca2+ homeostasis at dendritic spines in hippocampal neurons. *J Neurosci, 25*(18), 4587-4592. doi:10.1523/jneurosci.4822-04.2005

Scarisbrick, I. A., Radulovic, M., Burda, J. E., Larson, N., Blaber, S. I., Giannini, C., . . . Vandell, A. G. (2012). Kallikrein 6 is a novel molecular trigger of reactive astrogliosis. *Biol Chem, 393*(5), 355-367. doi:10.1515/hsz-2011-0241

Sengupta, P. (2013). The Laboratory Rat: Relating Its Age With Human's. *Int J Prev Med, 4*(6), 624-630.

Shannon, P., Markiel, A., Ozier, O., Baliga, N. S., Wang, J. T., Ramage, D., . . . Ideker, T. (2003). Cytoscape: a software environment for integrated models of biomolecular interaction networks. *Genome Res, 13*(11), 2498-2504. doi:10.1101/gr.1239303

Shimamura, M., Taniyama, Y., Katsuragi, N., Koibuchi, N., Kyutoku, M., Sato, N., . . . Morishita, R. (2012). Role of central nervous system periostin in cerebral ischemia. *Stroke, 43*(4), 1108-1114. doi:10.1161/strokeaha.111.636662

Socodato, R., Portugal, C. C., Canedo, T., Rodrigues, A., Almeida, T. O., Henriques, J. F., . . . Relvas, J. B. (2020). Microglia Dysfunction Caused by the Loss of Rhoa Disrupts Neuronal Physiology and Leads to Neurodegeneration. *Cell Rep, 31*(12), 107796. doi:10.1016/j.celrep.2020.107796

Spear, L. P. (2016). Alcohol Consumption in Adolescence: a Translational Perspective. *Current Addiction Reports, 3*(1), 50-61. doi:10.1007/s40429-016-0088-9

Spear, L. P., & Swartzwelder, H. S. (2014a). Adolescent alcohol exposure and persistence of adolescent-typical phenotypes into adulthood: a mini-review. *Neurosci Biobehav Rev, 45*, 1-8. doi:10.1016/j.neubiorev.2014.04.012

Spear, L. P., & Swartzwelder, H. S. (2014b). Adolescent alcohol exposure and persistence of adolescent-typical phenotypes into adulthood: A mini-review. *Neurosci Biobehav Rev*. doi:10.1016/j.neubiorev.2014.04.012

Stogsdill, J. A., Ramirez, J., Liu, D., Kim, Y. H., Baldwin, K. T., Enustun, E., . . . Eroglu, C. (2017). Astrocytic neuroligins control astrocyte morphogenesis and synaptogenesis. *Nature, 551*(7679), 192-197. doi:10.1038/nature24638

Subramanian, A., Tamayo, P., Mootha, V. K., Mukherjee, S., Ebert, B. L., Gillette, M. A., . . . Mesirov, J. P. (2005). Gene set enrichment analysis: A knowledge-based approach for interpreting genome-wide expression profiles. *Proceedings of the National Academy of Sciences, 102*(43), 15545-15550. doi:10.1073/pnas.0506580102

Swartzwelder, H. S., Risher, M. L., Miller, K. M., Colbran, R. J., Winder, D. G., & Wills, T. A. (2016). Changes in the Adult GluN2B Associated Proteome following Adolescent Intermittent Ethanol Exposure. *PLoS One, 11*(5), e0155951. doi:10.1371/journal.pone.0155951

Tanner, M. R., Pennington, M. W., Laragione, T., Gulko, P. S., & Beeton, C. (2017). KCa1.1 channels regulate β(1)-integrin function and cell adhesion in rheumatoid arthritis fibroblast-like synoviocytes. *Faseb j, 31*(8), 3309-3320. doi:10.1096/fj.201601097R

Tapert, S. F., Baratta, M. V., Abrantes, A. M., & Brown, S. A. (2002). Attention dysfunction predicts substance involvement in community youths. *J Am Acad Child Adolesc Psychiatry, 41*(6), 680-686. doi:10.1097/00004583-200206000-00007

Tapert, S. F., & Brown, S. (1999). Neuropsychological correlates of adolescent substance abuse: four-year outcomes. *Journal of the International Neuropsychological Society : JINS, 5*(6), 481-493.

The Gene Ontology, C. (2019). The Gene Ontology Resource: 20 years and still GOing strong. *Nucleic Acids Res, 47*(D1), D330-D338. doi:10.1093/nar/gky1055

U.S. DOJ. (2005). Drinking In America: Myths, Realities, and Prevention Policy. *Juvenile Justice Clearinghouse/NCJRS.*

Van Wagoner, N. J., & Benveniste, E. N. (1999). Interleukin-6 expression and regulation in astrocytes. *J Neuroimmunol, 100*(1-2), 124-139. doi:10.1016/s0165-5728(99)00187-3

Vetreno, R. P., & Crews, F. T. (2015). Binge ethanol exposure during adolescence leads to a persistent loss of neurogenesis in the dorsal and ventral hippocampus that is associated with impaired adult cognitive functioning. *Front Neurosci, 9*, 35. doi:10.3389/fnins.2015.00035

Vetreno, R. P., & Crews, F. T. (2018). Adolescent binge ethanol-induced loss of basal forebrain cholinergic neurons and neuroimmune activation are prevented by exercise and indomethacin. *PLoS One, 13*(10), e0204500. doi:10.1371/journal.pone.0204500

Wang, L., Du, F., & Wang, X. (2008). TNF-alpha induces two distinct caspase-8 activation pathways. *Cell, 133*(4), 693-703. doi:10.1016/j.cell.2008.03.036

Weinlich, R., & Green, D. R. (2014). The two faces of receptor interacting protein kinase-1. *Mol Cell, 56*(4), 469-480. doi:10.1016/j.molcel.2014.11.001

Williams, M. E., Wilke, S. A., Daggett, A., Davis, E., Otto, S., Ravi, D., . . . Ghosh, A. (2011). Cadherin-9 regulates synapse-specific differentiation in the developing hippocampus. *Neuron, 71*(4), 640-655. doi:10.1016/j.neuron.2011.06.019

World Health Organization. (2018). *Global status report on alcohol and health 2018*. Retrieved from Switzerland:

Yan, H., Li, Q., Fleming, R., Madison, R. D., Wilson, W. A., & Swartzwelder, H. S. (2009). Developmental sensitivity of hippocampal interneurons to ethanol: involvement of the hyperpolarization-activated current, Ih. *J Neurophysiol, 101*(1), 67-83. doi:10.1152/jn.90557.2008

Yoon, H., Radulovic, M., & Scarisbrick, I. A. (2018). Kallikrein-related peptidase 6 orchestrates astrocyte form and function through proteinase activated receptor-dependent mechanisms. *Biol Chem, 399*(9), 1041-1052. doi:10.1515/hsz-2018-0122

Zhang, R. X., Han, Y., Chen, C., Xu, L. Z., Li, J. L., Chen, N., . . . Lu, L. (2016). EphB2 in the Medial Prefrontal Cortex Regulates Vulnerability to Stress. *Neuropsychopharmacology, 41*(10), 2541-2556. doi:10.1038/npp.2016.58

Zhang, X., Bertaso, F., Yoo, J. W., Baumgärtel, K., Clancy, S. M., Lee, V., . . . Jegla, T. (2010). Deletion of the potassium channel Kv12.2 causes hippocampal hyperexcitability and epilepsy. *Nat Neurosci, 13*(9), 1056-1058. doi:10.1038/nn.2610

FIGURES

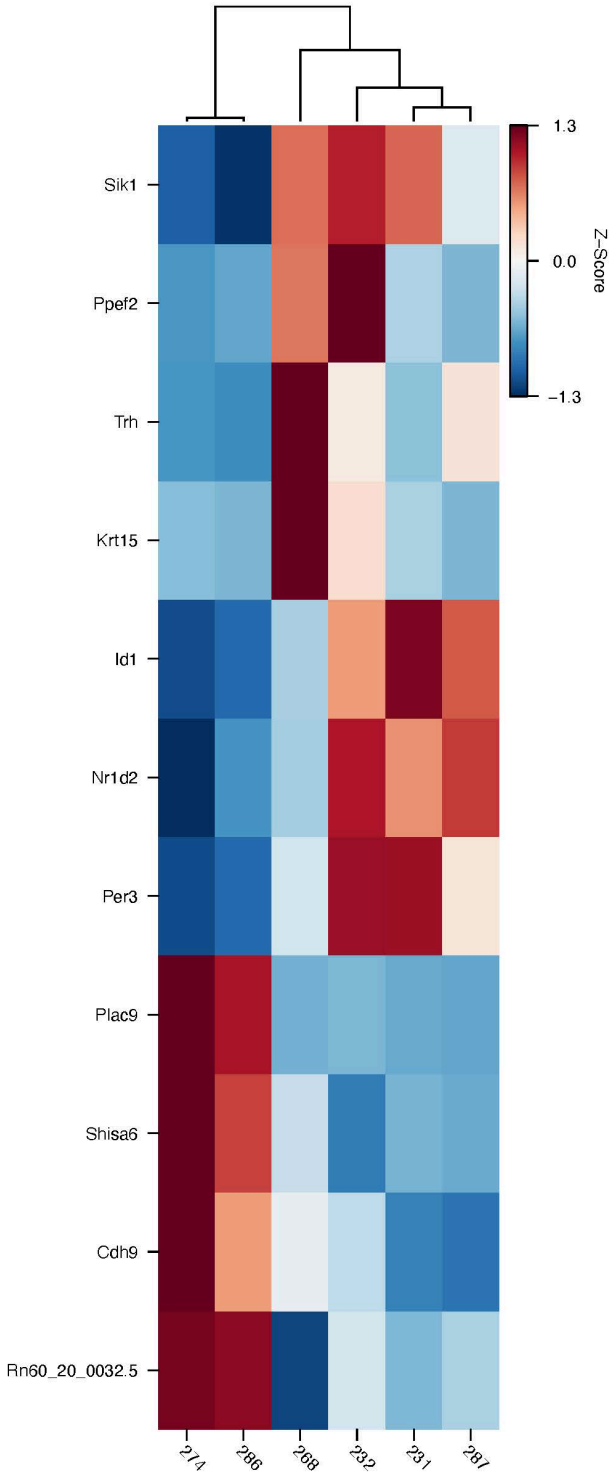

Figure 1. Heatmap of the differentially expressed genes (DEGs) with FDR≤0.05 for PND35 EtOH vs H_2O.

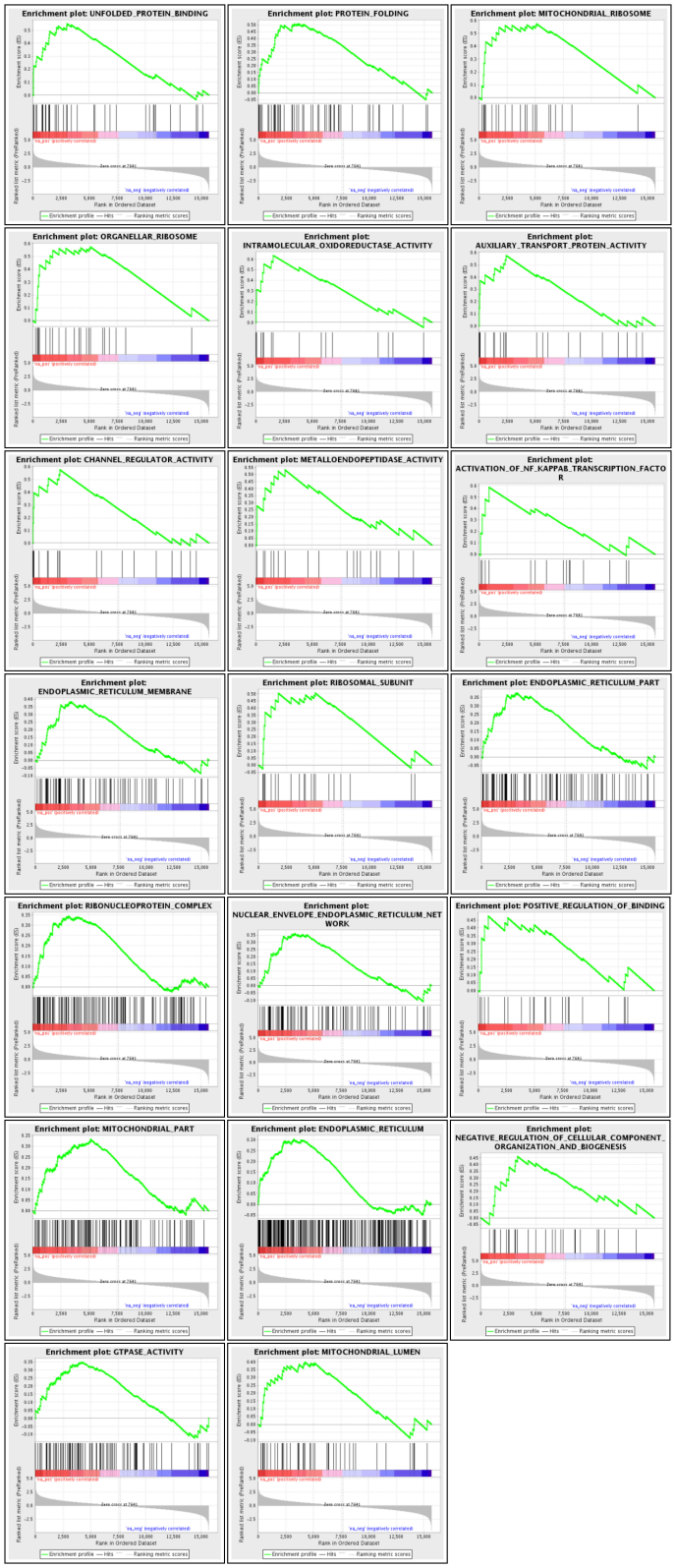

Figure 2. Top 20 enriched GO terms upregulated for PND35 EtOH vs H_2O.

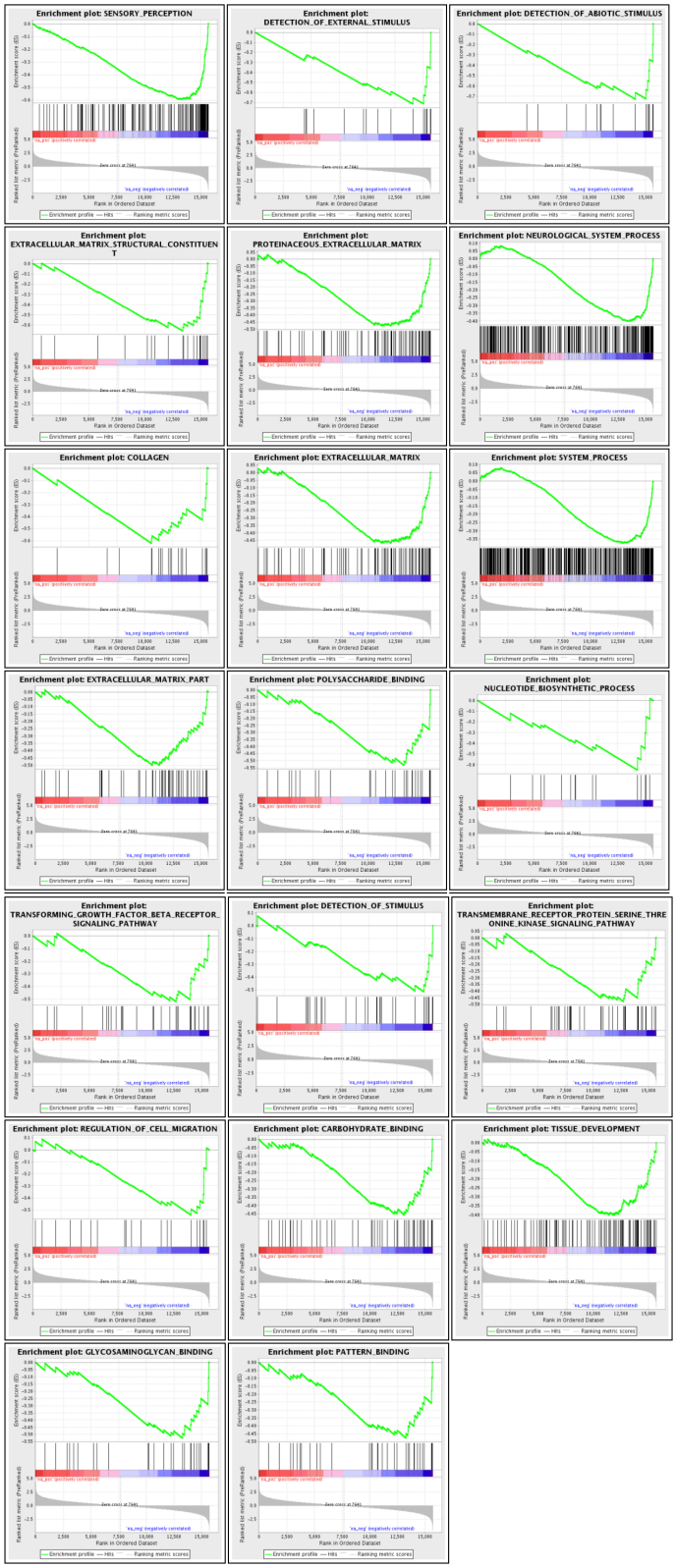

Figure 3. Top 20 enriched GO terms negatively regulated for PND35 EtOH vs H_2O.

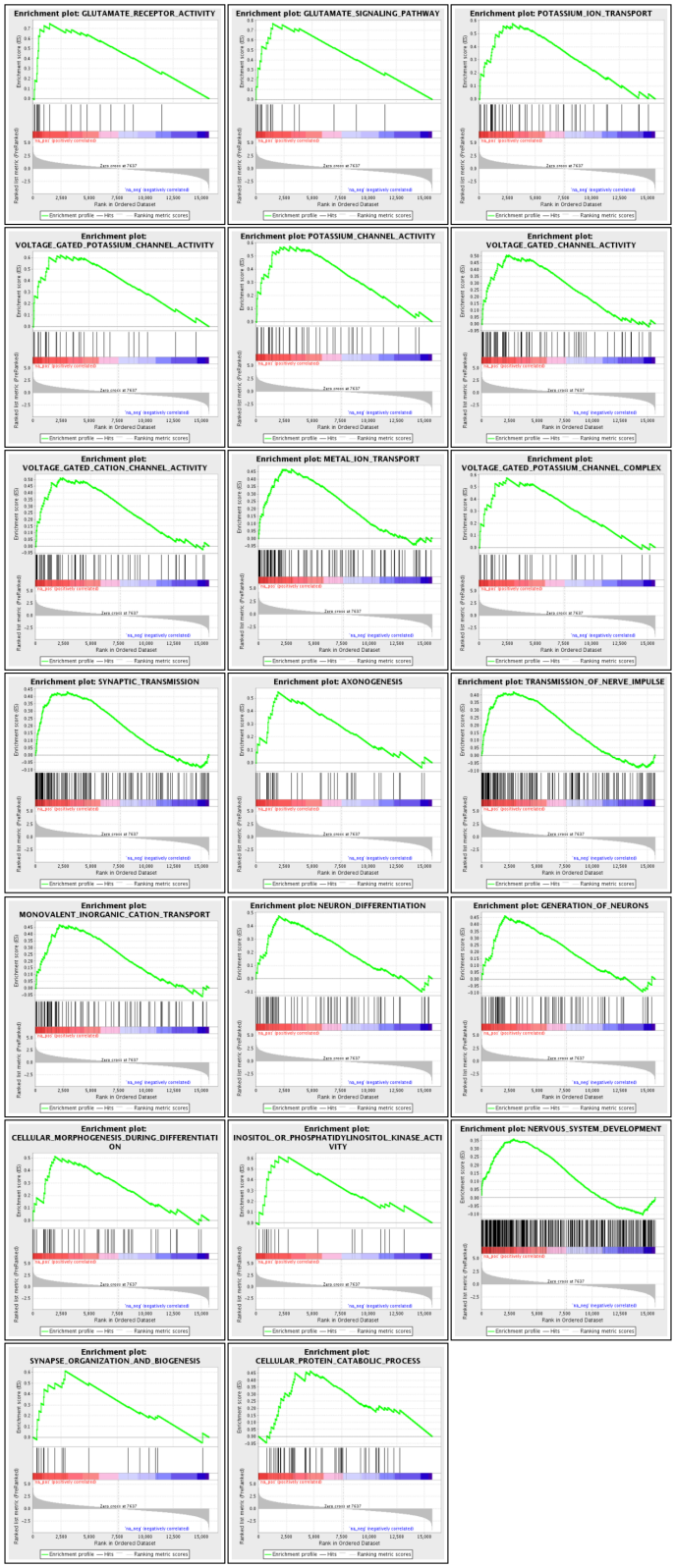

Figure 4. Top 20 enriched GO terms upregulated for PND46 EtOH vs H_2O.

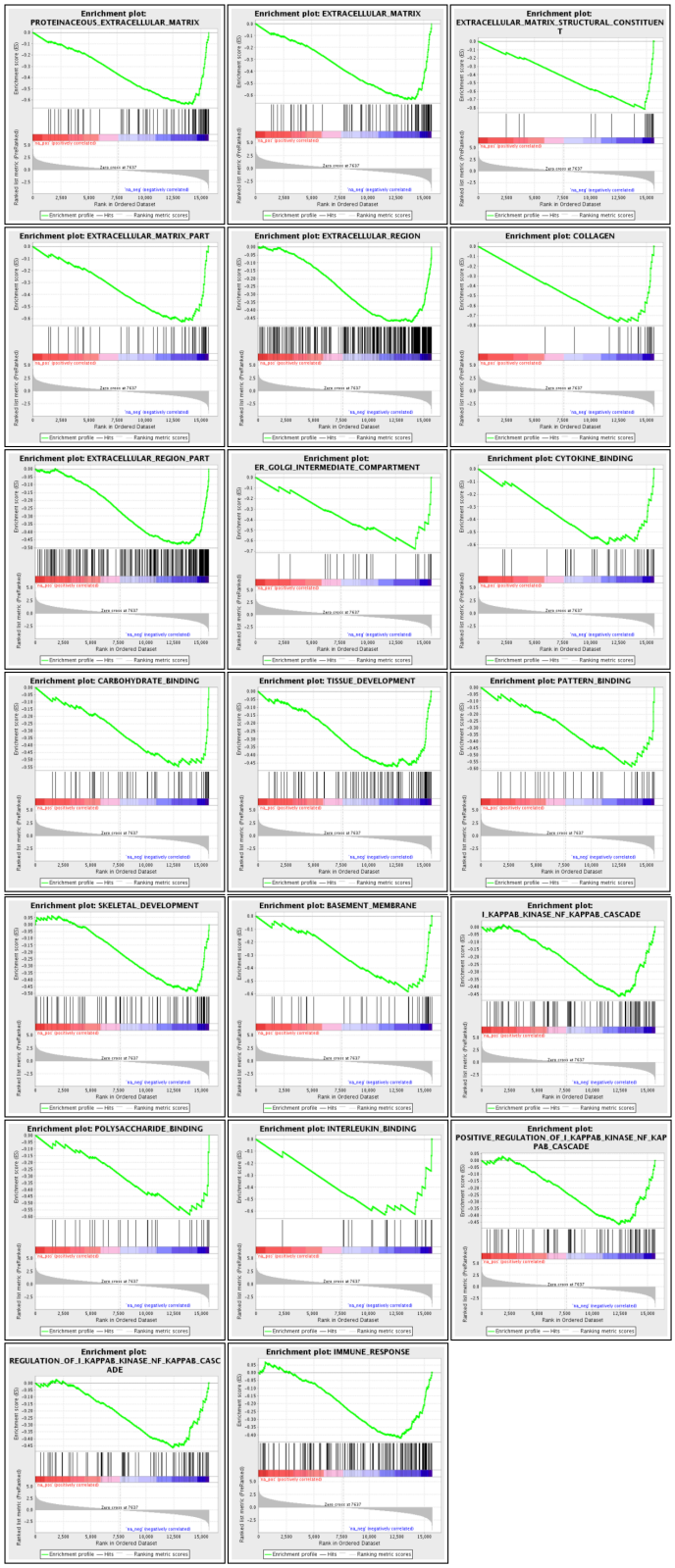

Figure 5. Top 20 enriched GO terms negatively regulated for PND46 EtOH vs H_2O.

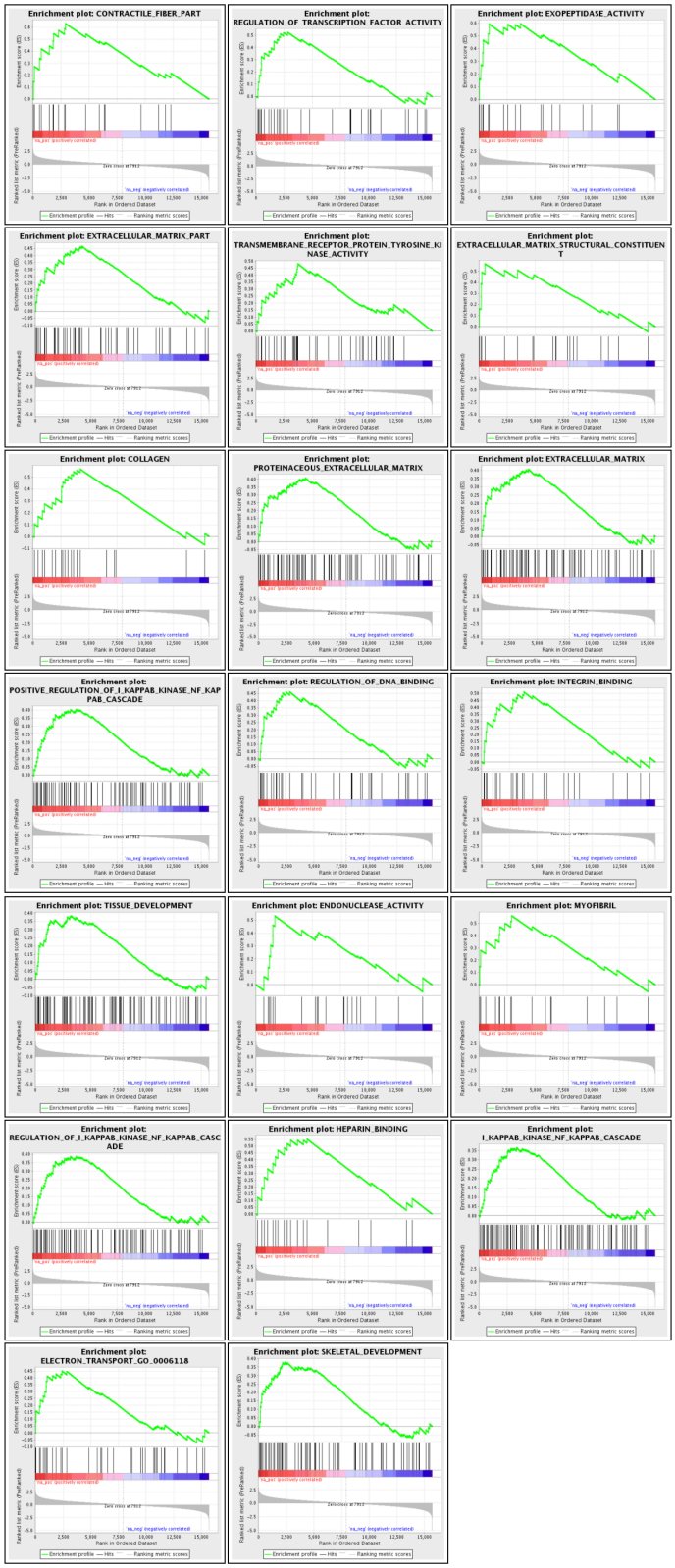

Figure 6. Top 20 enriched GO terms regulated for PND70 EtOH vs H_2O.

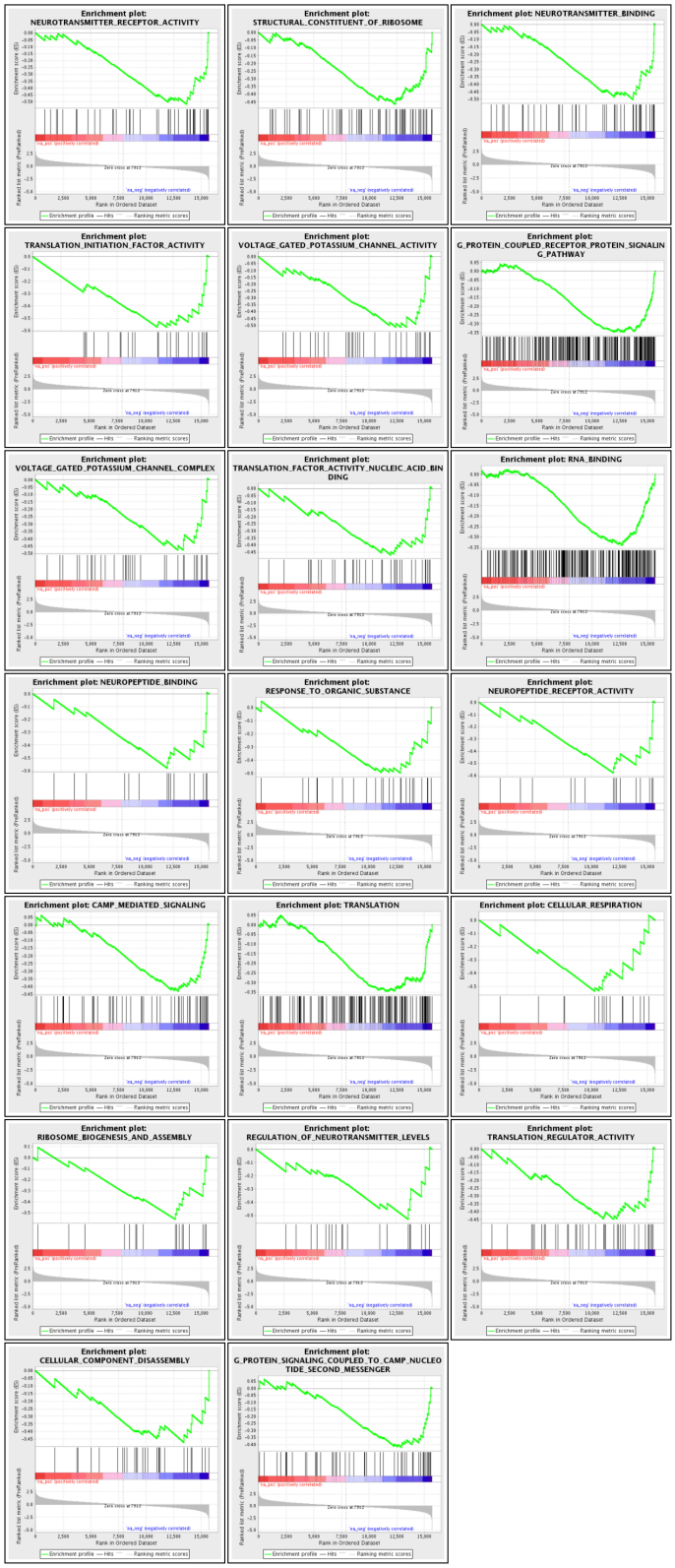

Figure 7. Top 20 enriched GO terms negatively regulated for PND70 EtOH vs H_2O.

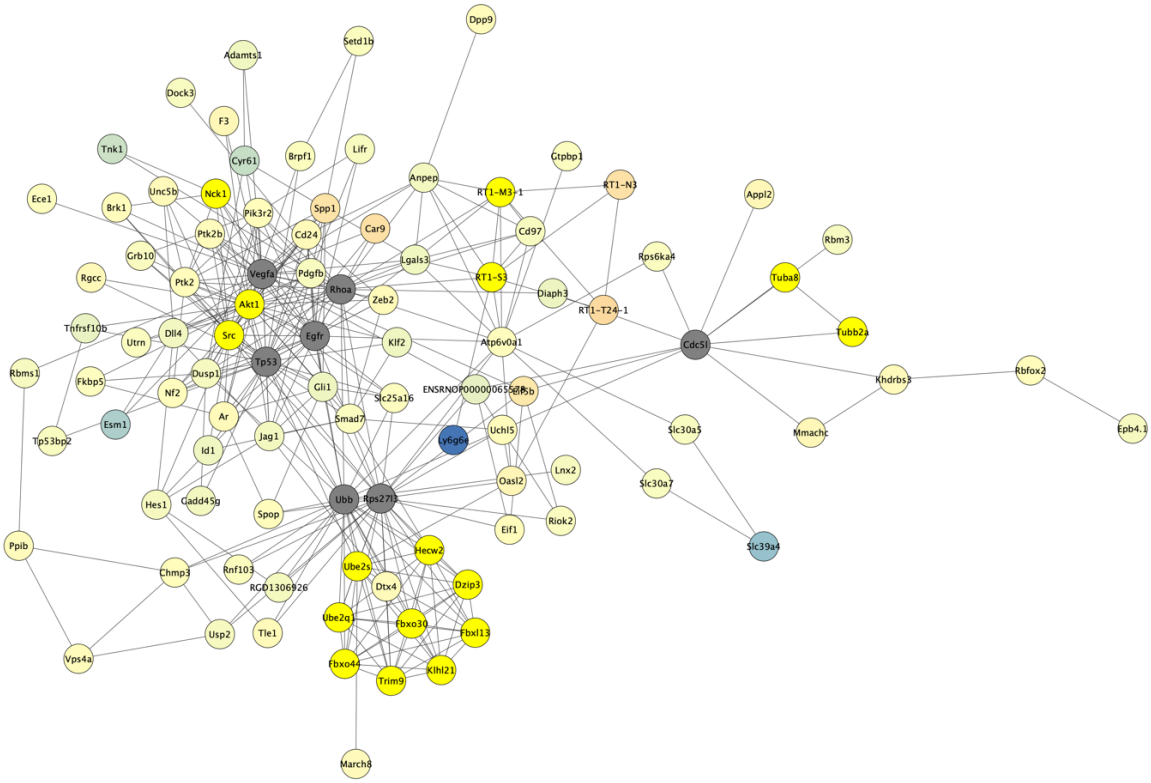

Figure 8. Adaptive immune system is one of top enriched functions under Reactome Pathways in cluster 1 for PND35 EtOH vs H_2O. The clusterMaker app (Morris *et al.*, 2011) identified 16 genes associated with the adaptive immune system (FDR=2.91×10^{-6}).

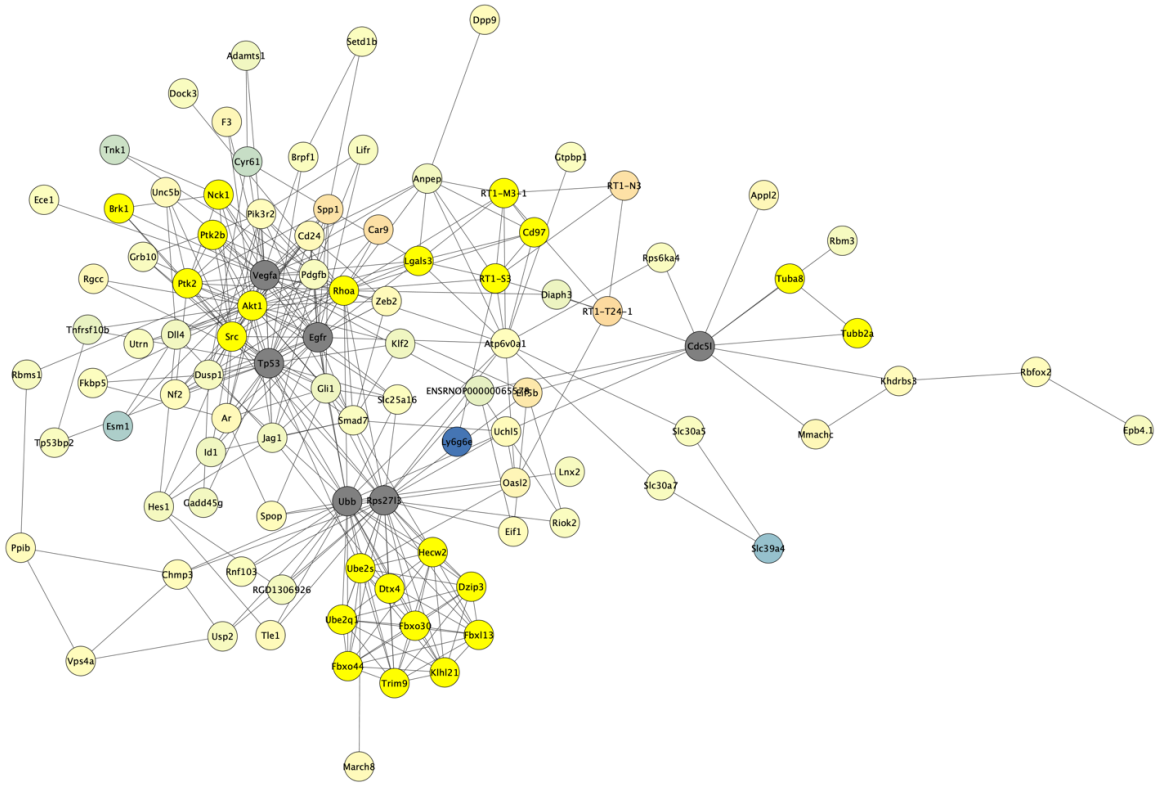

Figure 9. Immune system is one of top enriched functions under Reactome Pathways in cluster 1 for PND35 EtOH vs H_2O. The clusterMaker app (Morris *et al.*, 2011) identified 23 genes associated with the immune system (FDR=2.91×10^{-6}).

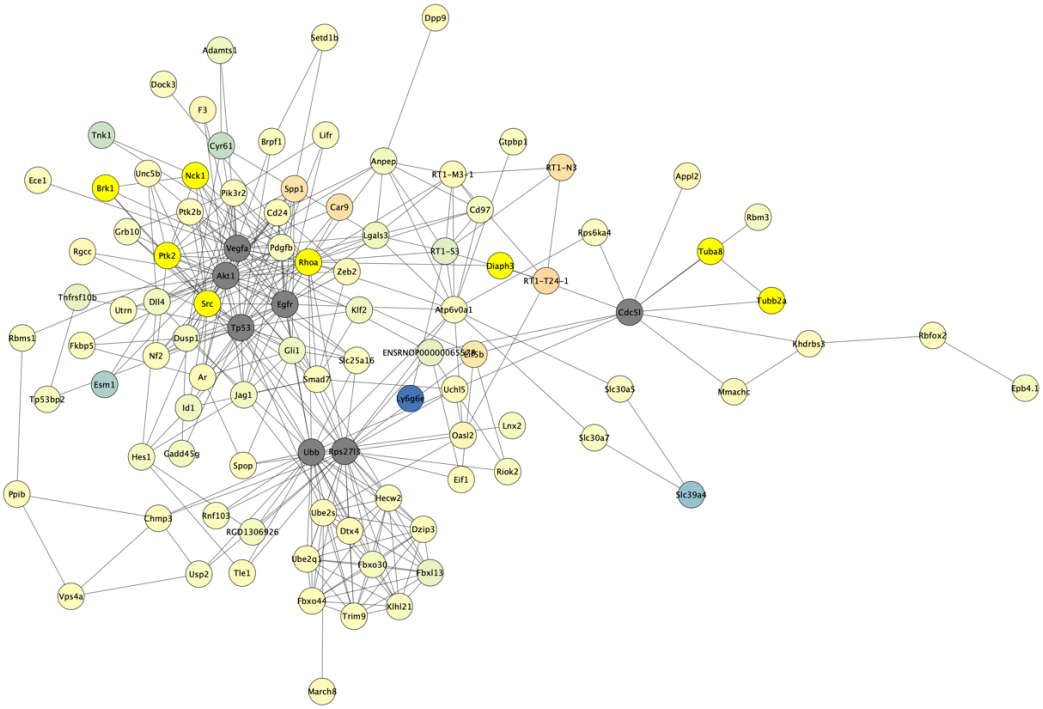

Figure 10. RHO GTPase effectors is one of top enriched functions under Reactome Pathways in cluster 1 for PND35 EtOH vs H_2O. The clusterMaker app (Morris *et al.*, 2011) identified 8 genes associated with the RHO GTPase effectors (FDR=$2.5x10^{-4}$).

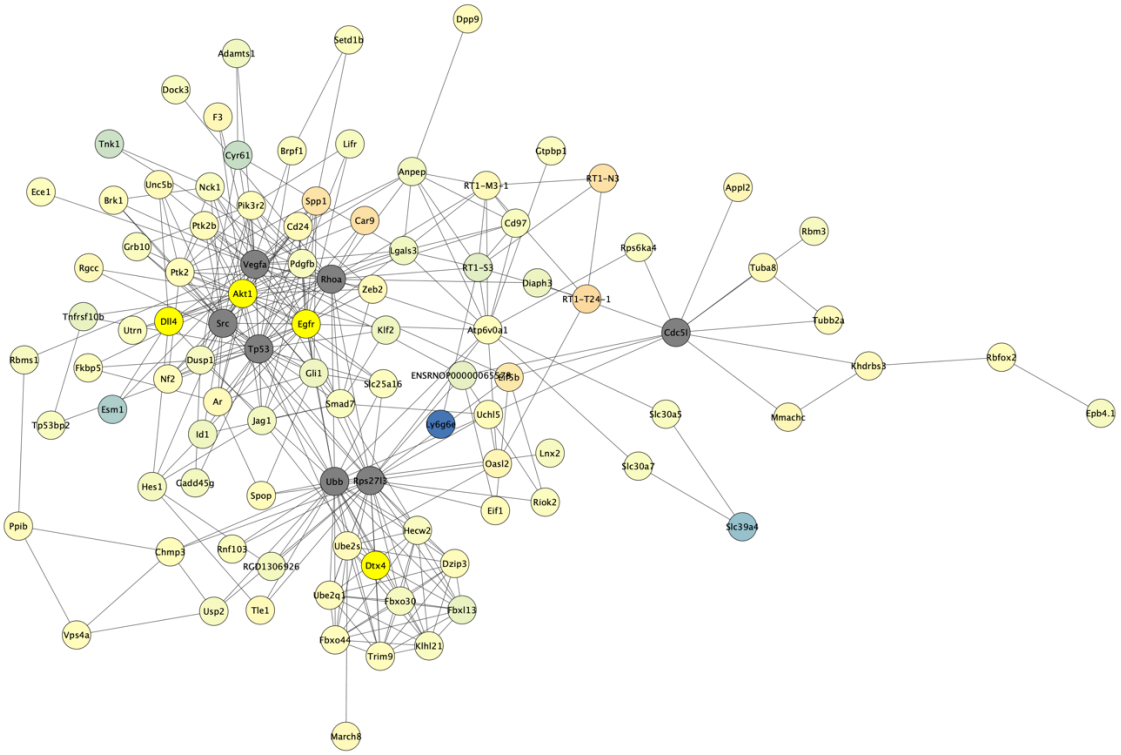

Figure 11. Signaling by NOTCH is one of top enriched functions under Reactome Pathways in cluster 1 for PND35 EtOH vs H_2O. The clusterMaker app (Morris *et al.*, 2011) identified 4 genes associated with Signaling by NOTCH (FDR=5.8x10^{-4}).

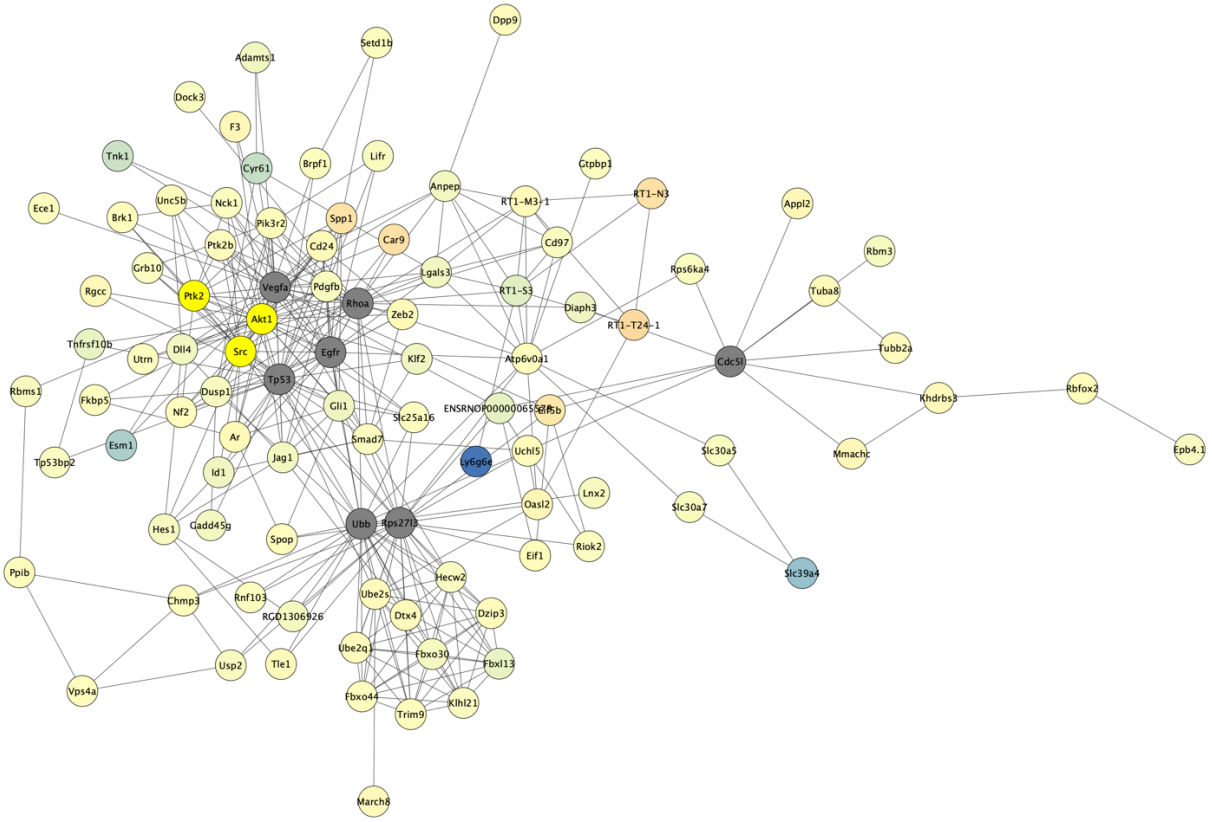

Figure 12. Integrin alphaIIb beta3 signaling is one of top enriched functions under Reactome Pathways in cluster 1 for PND35 EtOH vs H_2O. The clusterMaker app (Morris *et al.*, 2011) identified 3 genes associated with the integrin alphaIIb beta3 signaling (FDR=$1.9x10^{-3}$).

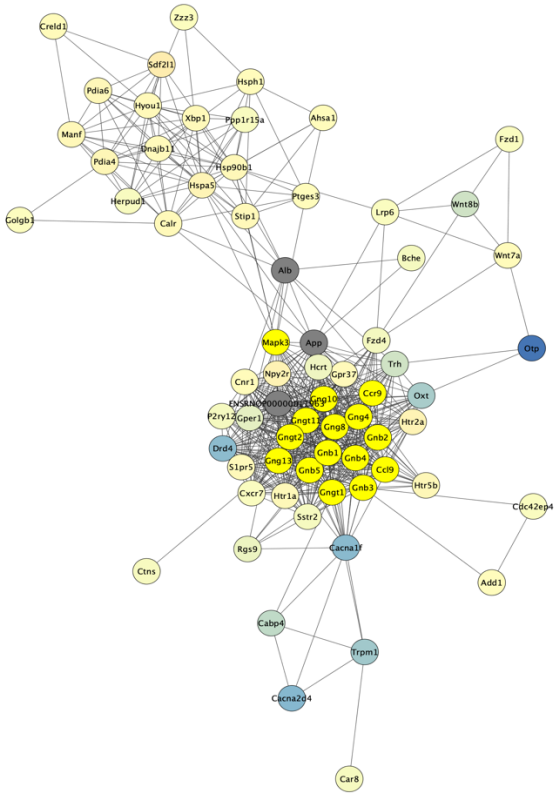

Figure 13. Chemokine signaling pathway is one of top enriched functions under Reactome Pathways in cluster 2 for PND35 EtOH vs H_2O. The clusterMaker app (Morris *et al.*, 2011) identified 15 genes associated with the chemokine signaling pathway (FDR=$1.42x10^{-16}$).

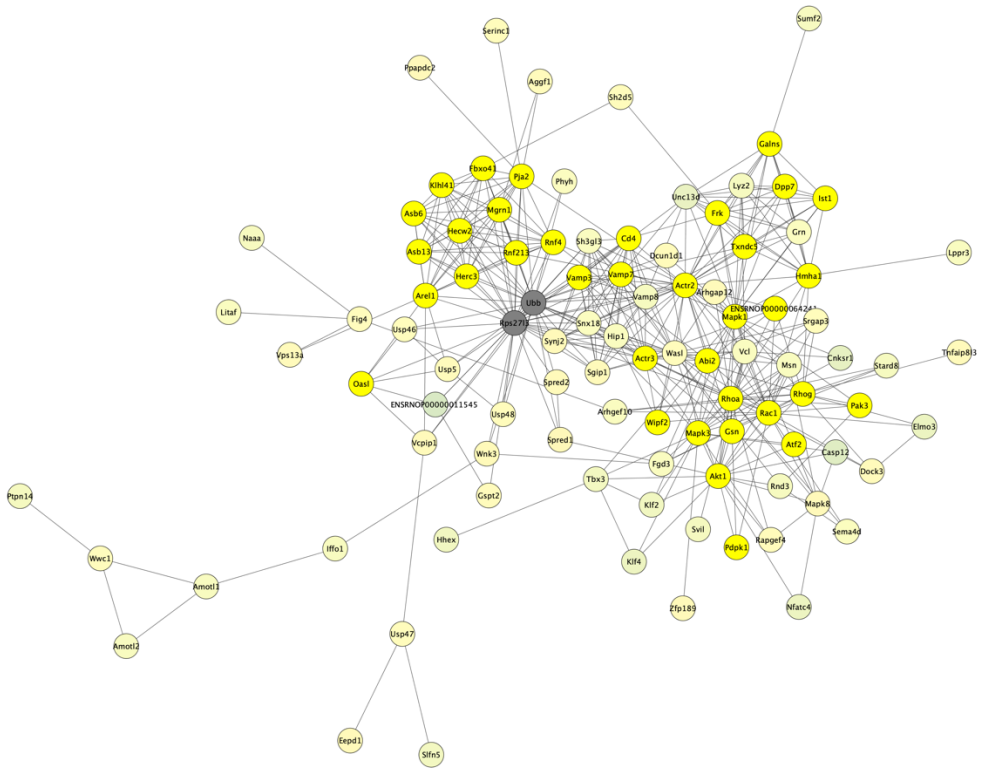

Figure 14. Immune system is one of top enriched functions under Reactome Pathways in cluster 1 for PND46 EtOH vs H_2O. The clusterMaker app (Morris *et al.*, 2011) identified 16 genes associated with the immune system (FDR=$1.18x10^{-16}$).

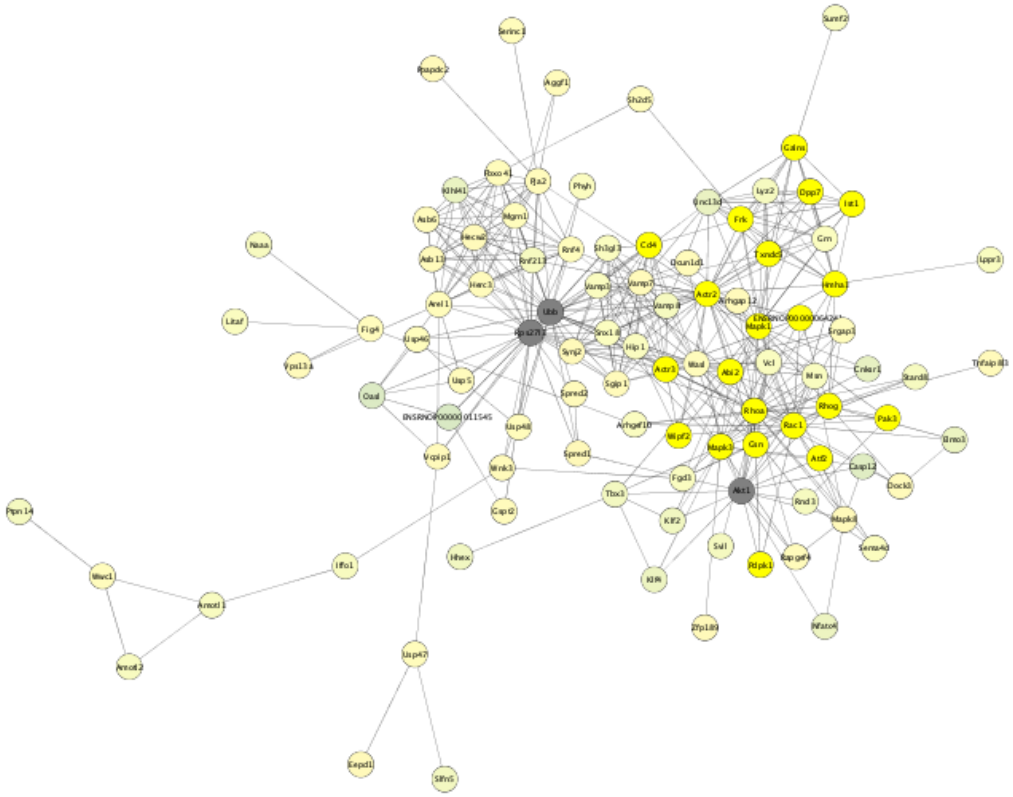

Figure 15. Innate immune system is one of top enriched functions under Reactome Pathways in cluster 1 for PND46 EtOH vs H_2O. The clusterMaker app (Morris *et al.*, 2011) identified 21 genes associated with the innate immune system (FDR=2.48×10^{-9}).

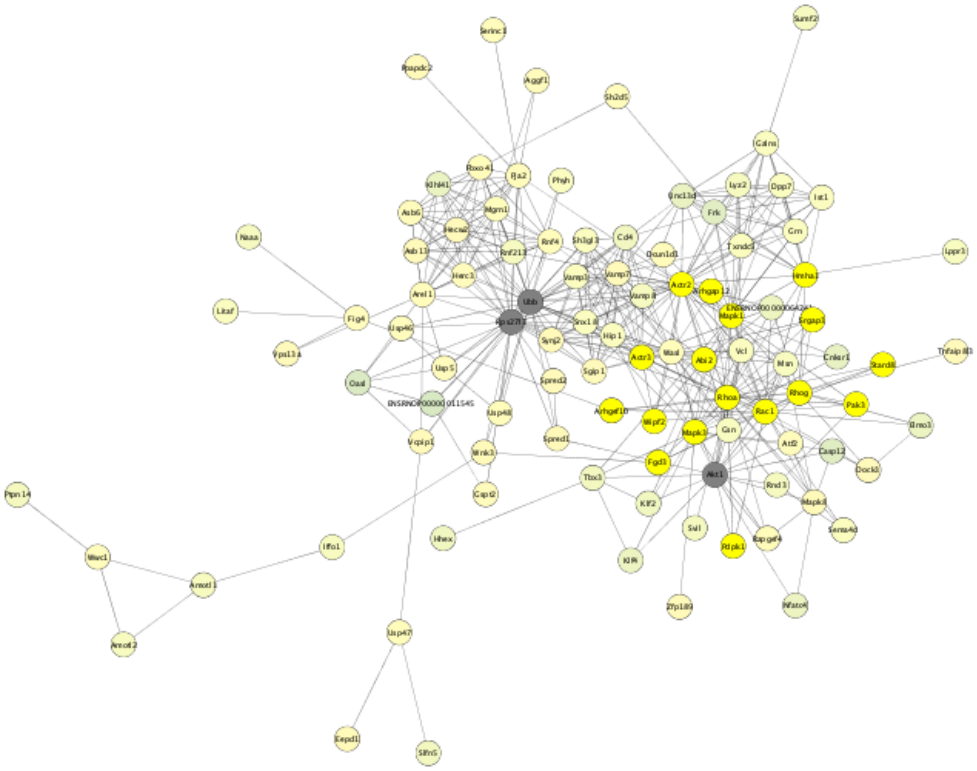

Figure 16. Signaling by Rho GTPases is one of top enriched functions under Reactome Pathways in cluster 1 for PND46 EtOH vs H_2O. The clusterMaker app (Morris *et al.*, 2011) identified 17 genes associated with the signaling by Rho GTPases (FDR=2.19x10^{-11}).

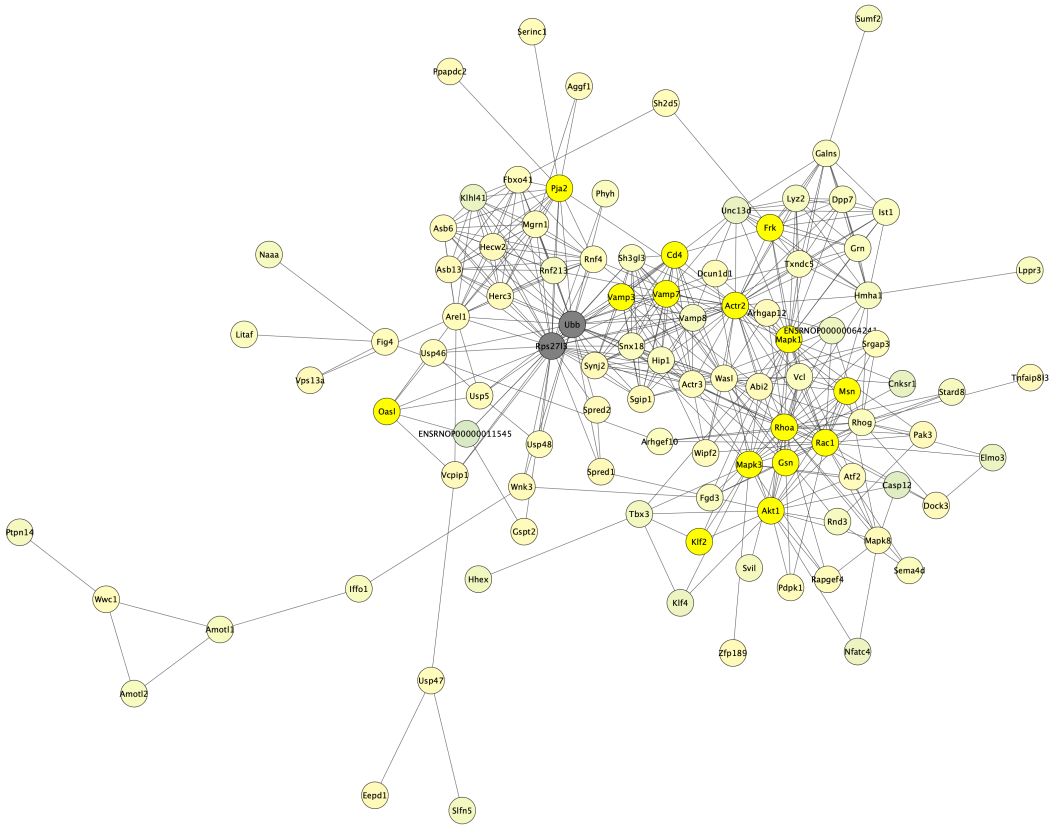

Figure 17. Immune system process is one of top enriched functions under GO Processes in cluster 1 for PND46 EtOH vs H_2O. The clusterMaker app (Morris *et al.*, 2011) identified 15 genes associated with the immune system process (FDR=$6.58x10^{-5}$).

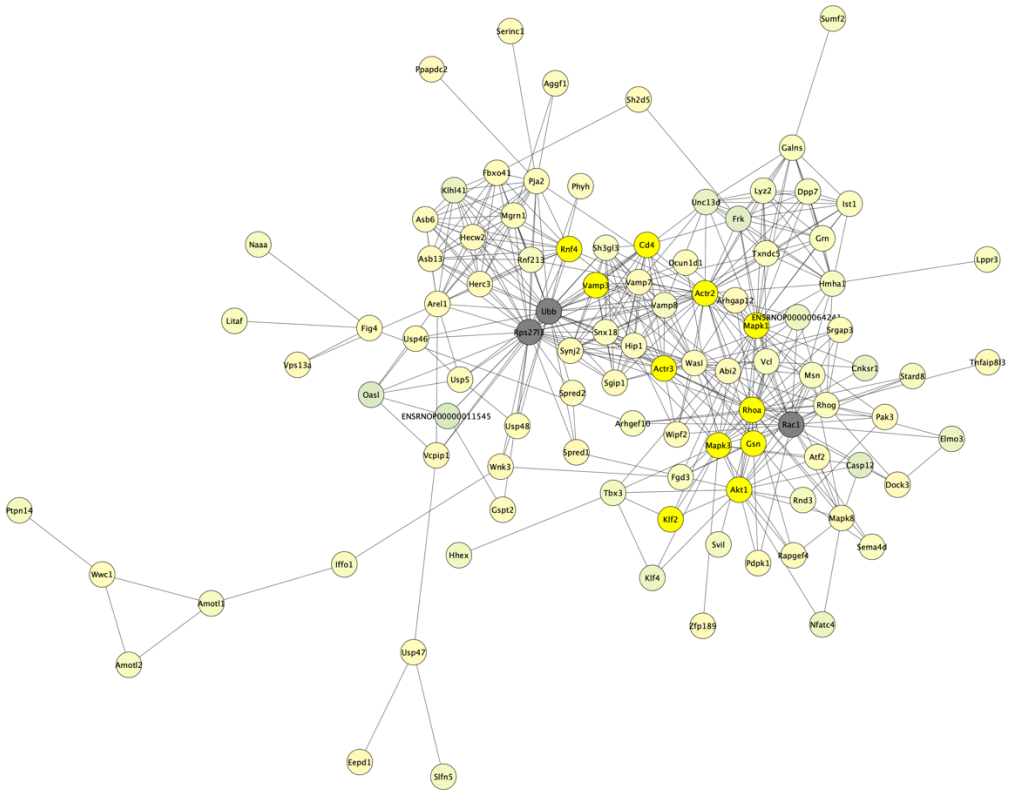

Figure 18. Cellular response to cytokine stimulus is one of top enriched functions under GO Processes in cluster 1 for PND46 EtOH vs H_2O. The clusterMaker app (Morris *et al.*, 2011) identified 11 genes associated with the cellular response to cytokine stimulus (FDR=$7.34x10^{-5}$).

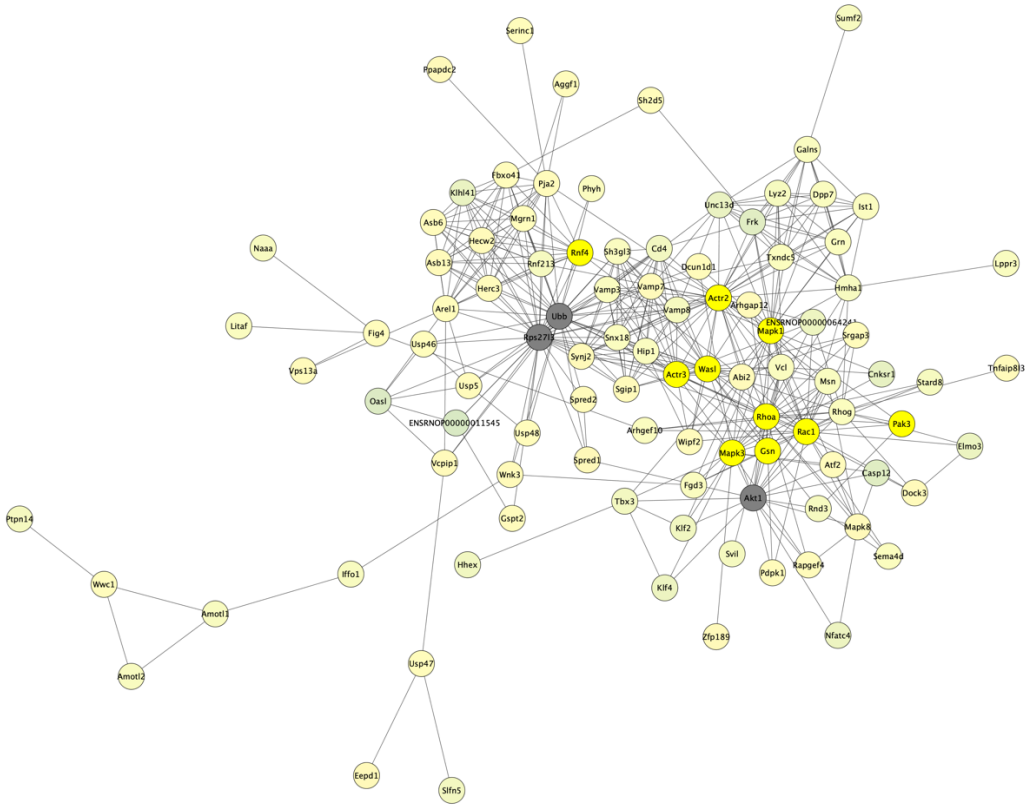

Figure 19. Regulation of cytoskeleton organization is one of top enriched functions under GO Processes in cluster 1 for PND46 EtOH vs H_2O. The clusterMaker app (Morris *et al.*, 2011) identified 10 genes associated with regulation of cytoskeleton organization (FDR=6.58×10^{-5}).

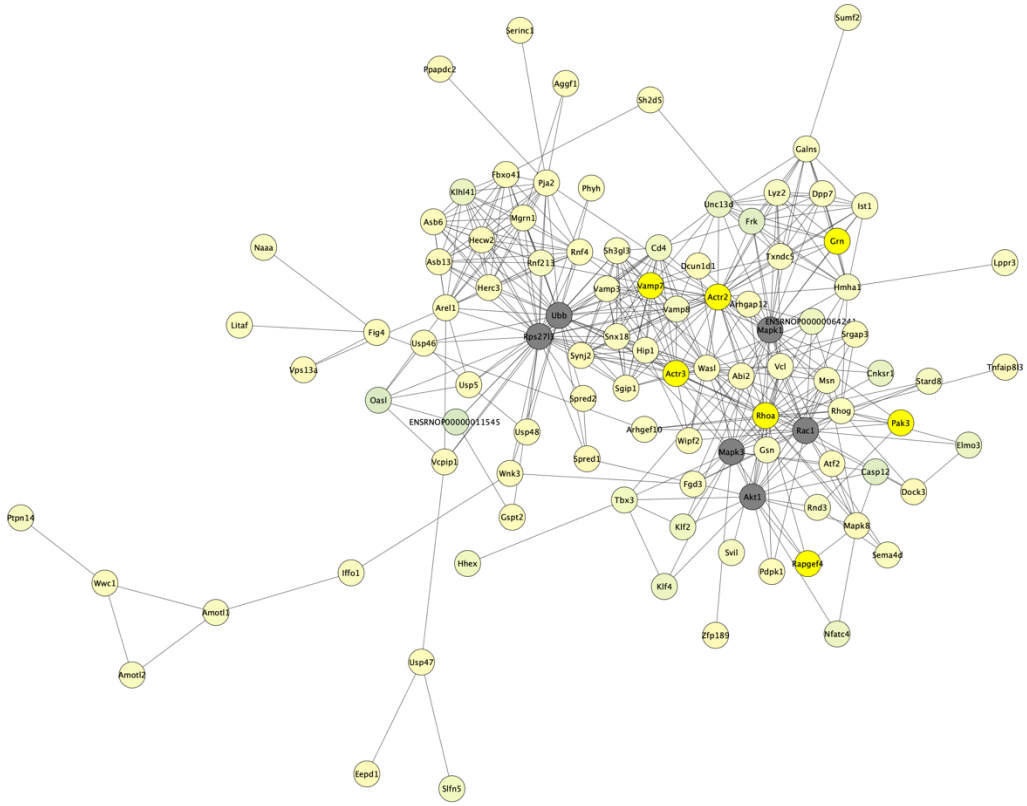

Figure 20. Regulation of dendrite development is one of top enriched functions under GO Processes in cluster 1 for PND46 EtOH vs H_2O. The clusterMaker app (Morris *et al.*, 2011) identified 7 genes associated with regulation of dendrite development (FDR=9.25×10^{-5}).

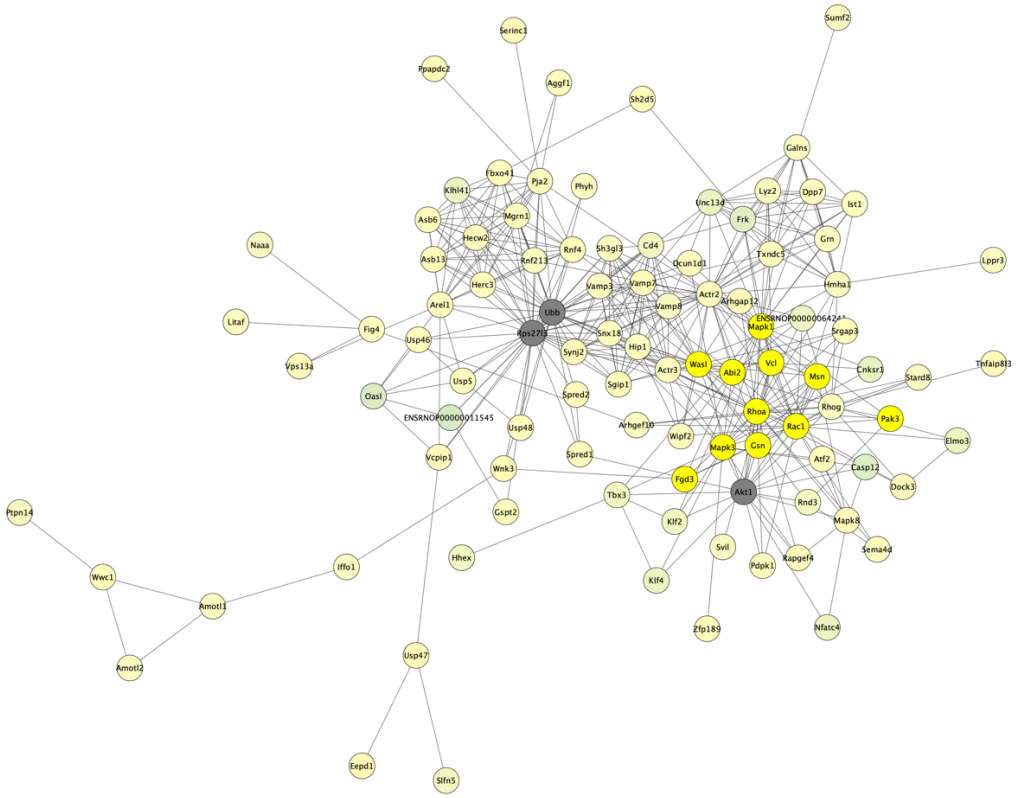

Figure 21. Regulation of actin cytoskeleton is one of top enriched functions under KEGG Pathways in cluster 1 for PND46 EtOH vs H_2O. The clusterMaker app (Morris *et al.*, 2011) identified 11 genes associated with regulation of actin cytoskeleton (FDR=$3.77x10^{-7}$).

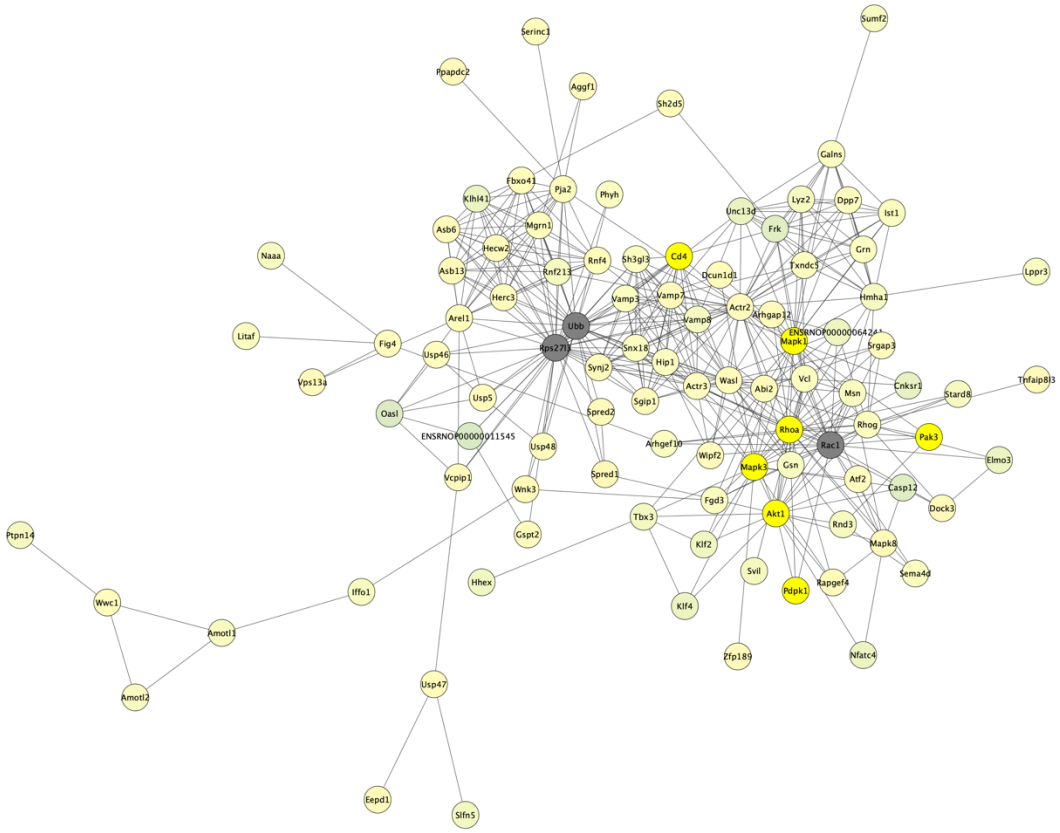

Figure 22. T cell receptor signaling pathways is one of top enriched functions under KEGG Pathways in cluster 1 for PND46 EtOH vs H_2O. The clusterMaker app (Morris *et al.*, 2011) identified 7 genes associated with T cell receptor signaling pathways (FDR=$1.21x10^{-5}$).

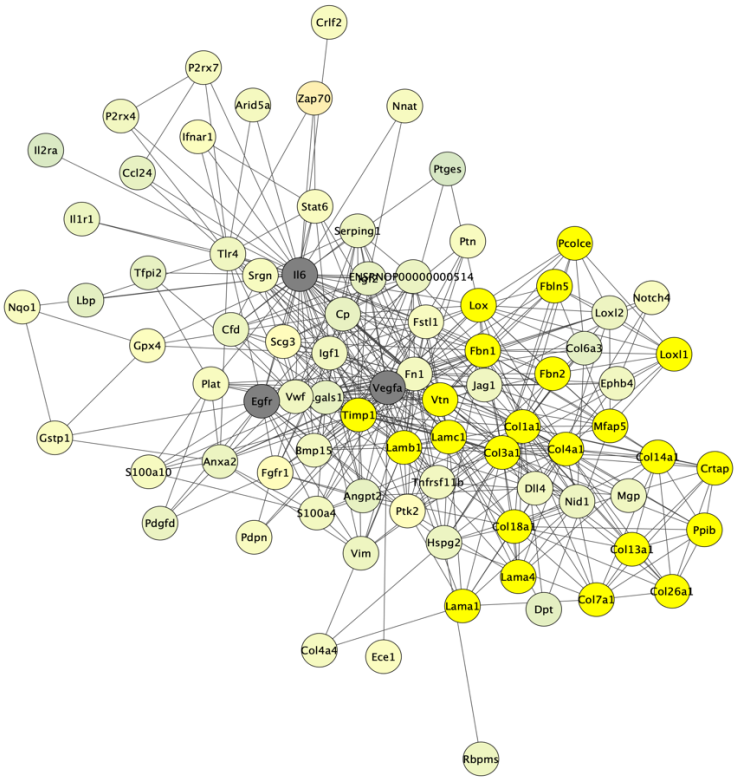

Figure 23. Extracellular matrix organization is one of top enriched functions under Reactome Pathways in cluster 2 for PND46 EtOH vs H_2O. The clusterMaker app (Morris *et al.*, 2011) identified 23 genes associated with extracellular matrix organization (FDR=7.93×10^{-25}).

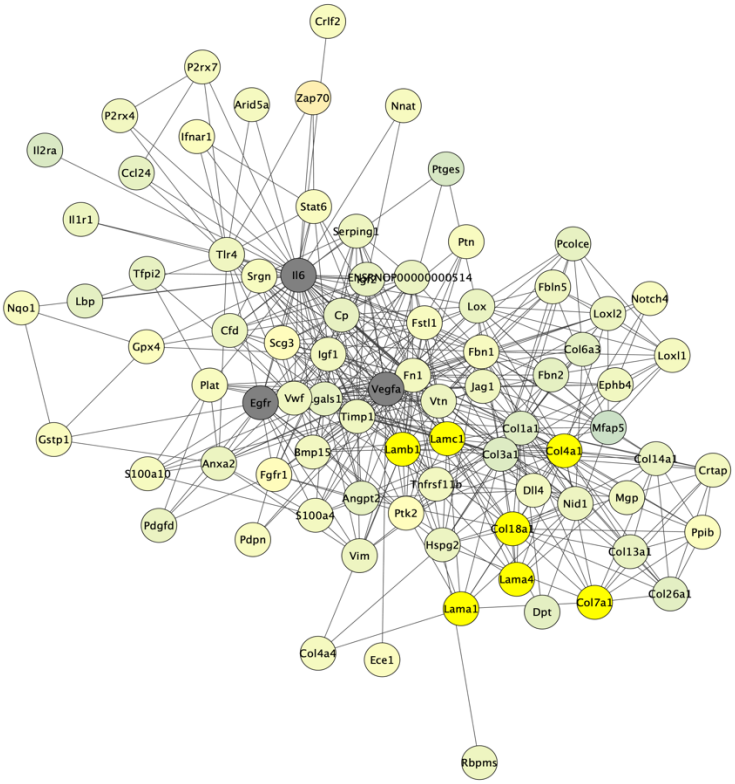

Figure 24. Laminin interactions is one of top enriched functions under Reactome Pathways in cluster 2 for PND46 EtOH vs H_2O. The clusterMaker app (Morris *et al.*, 2011) identified 7 genes associated with laminin interactions (FDR=1.19×10^{-10}).

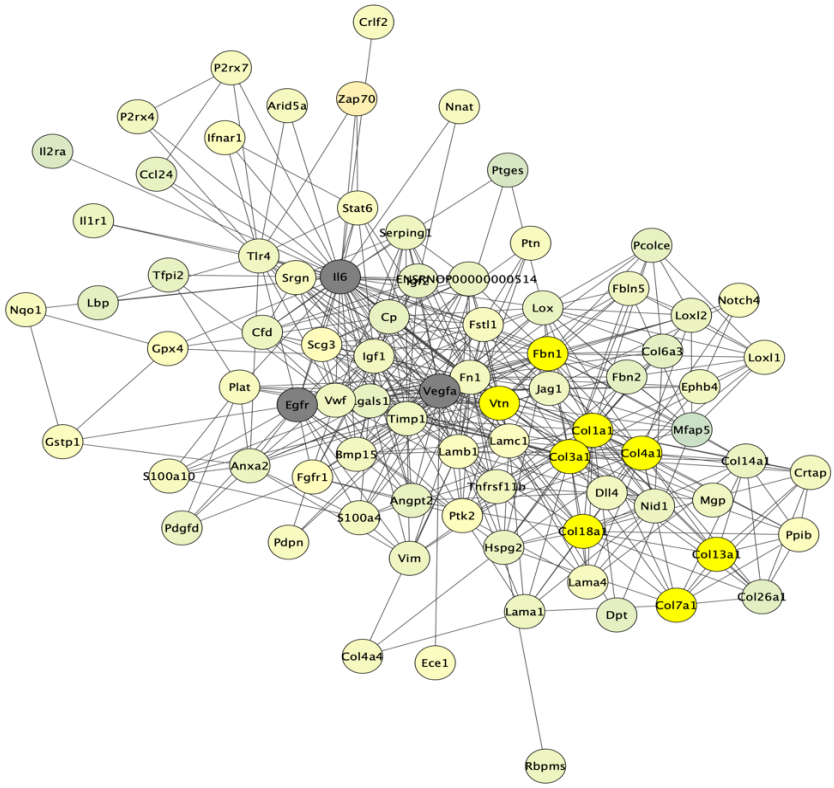

Figure 25. Integrin cell surface interactions is one of top enriched functions under Reactome Pathways in cluster 2 for PND46 EtOH vs H_2O. The clusterMaker app (Morris *et al.*, 2011) identified 8 genes associated with Integrin cell surface interactions (FDR=$1.34x10^{-9}$).

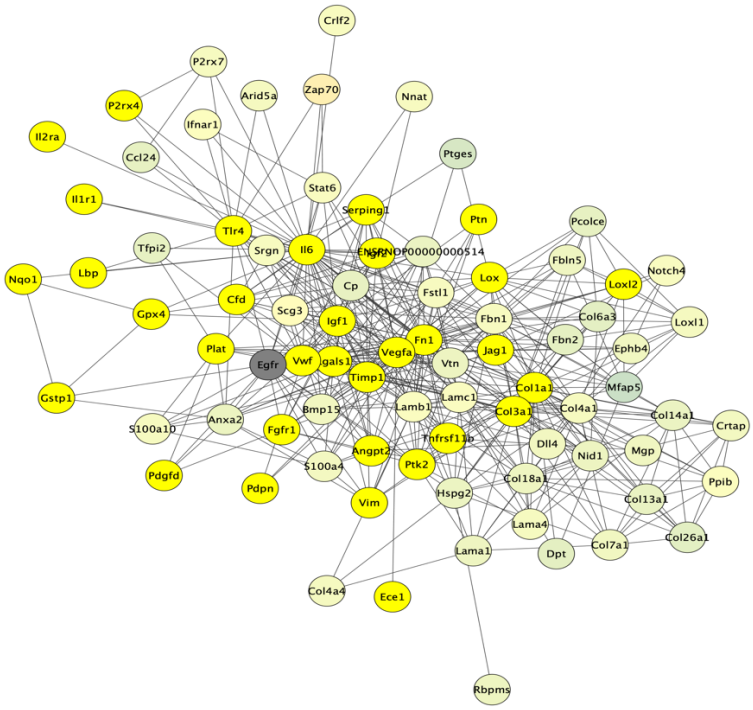

Figure 26. Response to stress is one of top enriched functions under GO Processes in cluster 2 for PND46 EtOH vs H_2O. The clusterMaker app (Morris *et al.*, 2011) identified 33 genes associated with response to stress (FDR=3.02×10^{-14}).

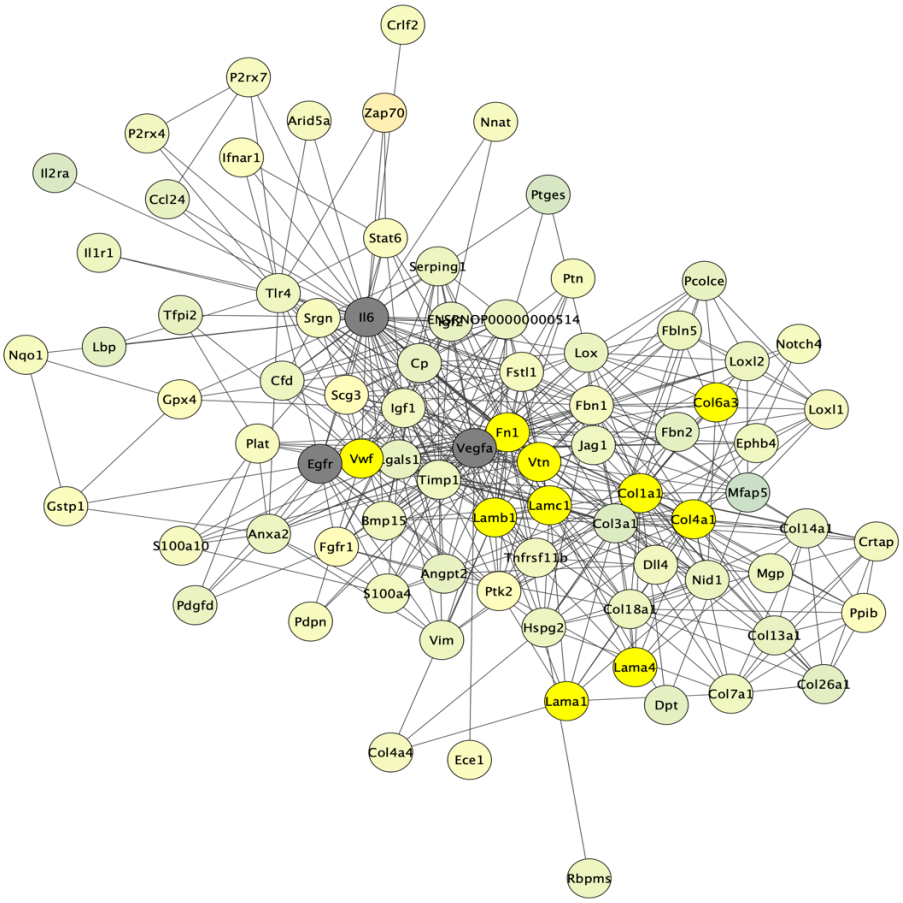

Figure 27. ECM-receptor interactions is one of top enriched functions under KEGG Pathways in cluster 2 for PND46 EtOH vs H_2O. The clusterMaker app (Morris *et al.*, 2011) identified 10 genes associated with ECM-receptor interactions (FDR=$8.39x10^{-12}$).

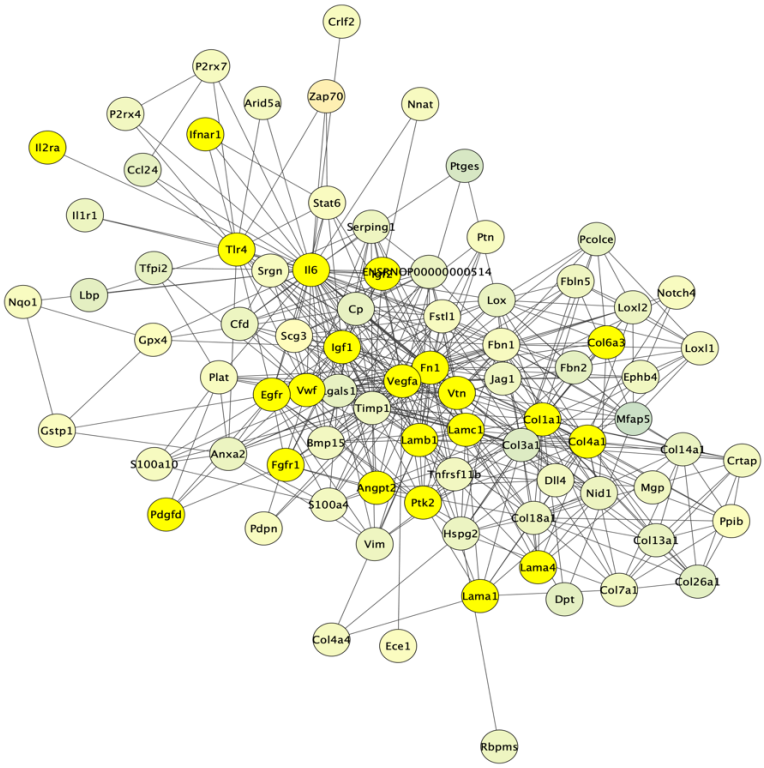

Figure 27. PI3K-Akt signaling pathway is one of top enriched functions under KEGG Pathways in cluster 2 for PND46 EtOH vs H_2O. The clusterMaker app (Morris *et al.*, 2011) identified 22 genes associated with PI3K-Akt signaling pathway (FDR=$1.52x10^{-19}$).

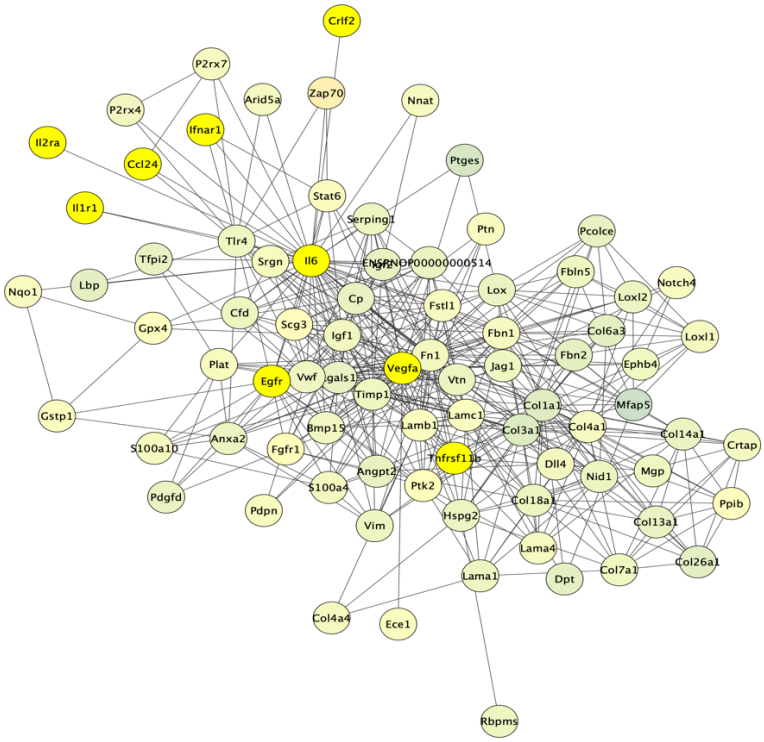

Figure 29. Cytokine-cytokine receptor interactions is one of top enriched functions under KEGG Pathways in cluster 2 for PND46 EtOH vs H_2O. The clusterMaker app (Morris *et al.*, 2011) identified 9 genes associated with cytokine-cytokine receptor interactions (FDR=$1.4x10^{-6}$).

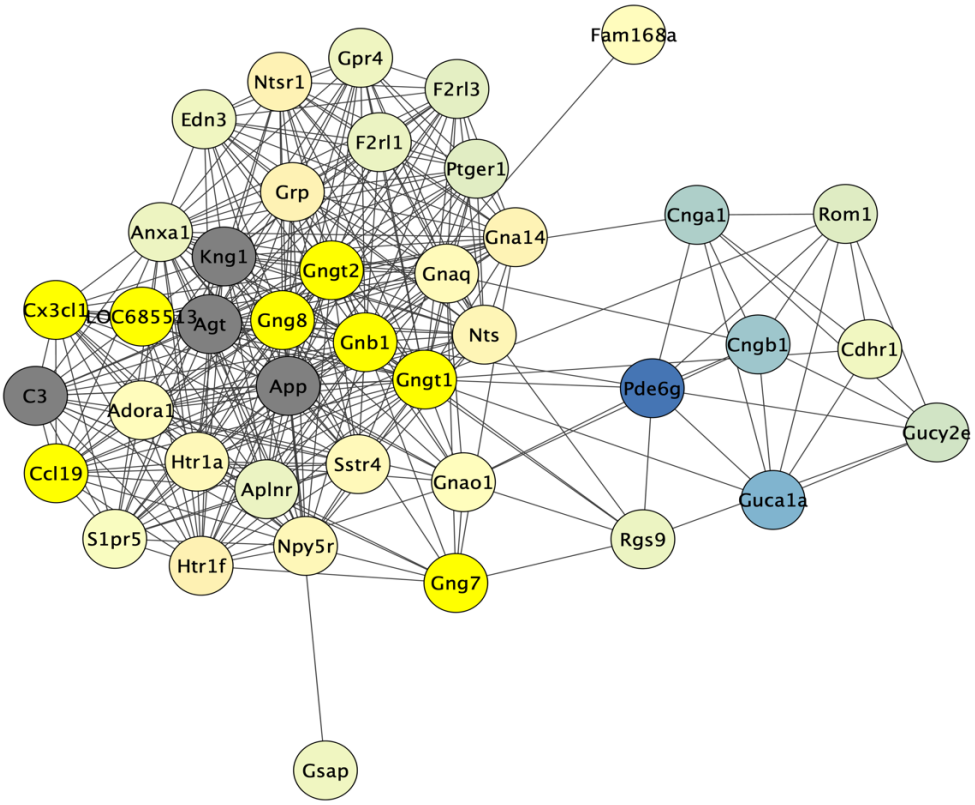

Figure 30. Chemokine signaling pathway is one of top enriched functions under KEGG Pathways in cluster 3 for PND46 EtOH vs H_2O. The clusterMaker app (Morris *et al.*, 2011) identified 8 genes associated with chemokine signaling pathway (FDR=4.95×10^{-9}).

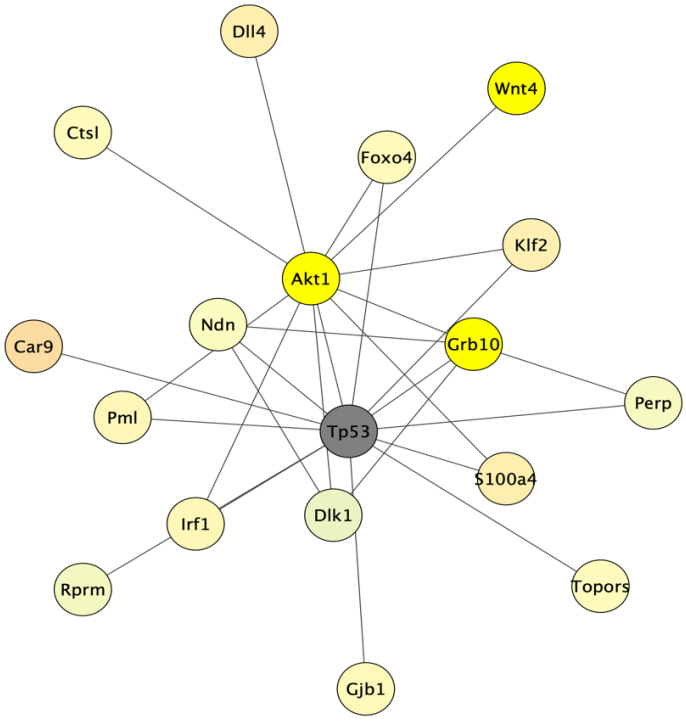

Figure 31. mTOR signaling pathway is one of top enriched functions under KEGG Pathways in cluster 2 for PND70 EtOH vs H_2O. The clusterMaker app (Morris *et al.*, 2011) identified 3 genes associated with mTOR signaling pathway (FDR=$1.9x10^{-3}$).

GSEA

	PND35	PND46	PND70
Remodeling	↓	↓↑	↑
Neuroimmune	–	↓	↑
Receptor Function	↓	↑	↓
K^+ Channels	↓↑	↑	↓

Cytoscape

	PND35	PND46	PND70
Remodeling	↑	↑	–
Neuroimmune	↑	↑	–
Receptor Function	↑	↑	–
K^+ Channels	–	–	–

Figure 32. Summary of pathway and enrichment analyses (GSEA and Cytoscape) exhibit temporal upregulation or downregulation of genes involved in remodeling, neuroimmune, receptor function, and K^+ channels. Blue arrows represent consistent results while red arrows represent contrasting results.